

Ring Opening Polymerization and Copolymerization of Cyclic Esters Catalyzed by Group 2 Metal Complexes Supported by Functionalized P–N Ligands

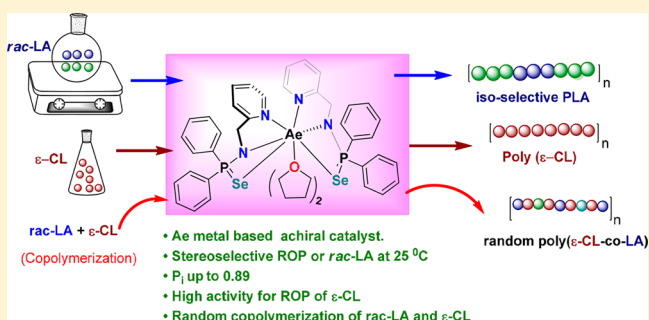
 Adimulam Harinath,[†] Jayeeta Bhattacharjee,[†] Alok Sarkar,[‡] Hari Pada Nayek,[§] and Tarun K. Panda^{*,†}
[†]Department of Chemistry, Indian Institute of Technology Hyderabad Kandi 502 285, Sangareddy, Telangana, India

[‡]Momentive Performance Materials Pvt. Ltd., Bangalore 560 100, India

[§]Department of Applied Chemistry, Indian Institute of Technology (ISM), Dhanbad 826 004, Jharkhand, India

Supporting Information

ABSTRACT: We report the preparation of alkali and alkaline earth (Ae) metal complexes supported by 2-picolyamino-diphenylphosphane chalcogenide $[(\text{Ph}_2\text{P}(=\text{E})\text{NCH}_2(\text{C}_5\text{H}_4\text{N}))]$ [E = S (**1-H**); Se (**2-H**)] ligands. The treatment of the protic ligand, **1-H** or **2-H**, with alkali metal hexamethyldisilazides at room temperature afforded the corresponding alkali metal salts $[\text{M}(\text{THF})_2(\text{Ph}_2\text{P}(=\text{E})\text{NCH}_2(\text{C}_5\text{H}_4\text{N}))]$ [M = Li, E = S (**3a**), Se (**3b**)] and $[\{\text{M}(\text{THF})_n(\text{Ph}_2\text{P}(=\text{E})\text{NCH}_2(\text{C}_5\text{H}_4\text{N}))_2\}]$ [M = Na, E = S (**4a**), Se (**4b**); M = K, E = Se (**5b**)] in good yield. The homoleptic Ae metal complexes $[\kappa^2-(\text{Ph}_2\text{P}(=\text{Se})\text{NCH}_2(\text{C}_5\text{H}_4\text{N}))\text{Mg}(\text{THF})]$ (**6b**) and $[\kappa^3-\{(\text{Ph}_2\text{P}(=\text{Se})\text{NCH}_2(\text{C}_5\text{H}_4\text{N}))_2\text{M}(\text{THF})_n\}]$ (M = Ca (**7b**), Sr (**8b**), Ba (**9b**)) were synthesized by the one-pot reaction of **2-H** with $[\text{KN}(\text{SiMe}_3)_2]$ and Ml_2 in a 2:2:1 molar ratio at room temperature. The molecular structures of the protic-ligands **1-H** and **2-H**, as well as complexes **3a,b**–**5a,b** and **6b**–**9b** were established using single-crystal X-ray analysis. The Ae metal complexes **6b**–**9b** were tested for ring-opening polymerization (ROP) of racemic lactide (*rac*-LA) and copolymerization of *rac*-LA and ϵ -caprolactone (ϵ -CL) at room temperature. In the ROP of *rac*-LA, the calcium complex **7b** exhibited high isoselectivity, with $P_i = 0.89$, whereas both the barium and strontium complexes showed lower isoselectivity with $P_i = 0.78$ – 0.62 . In the copolymerization of *rac*-LA and ϵ -CL, both barium and strontium complexes proved to be efficient precatalysts for the formation of the block copolymer *rac*-LA-CL, but the reactivity of **9b** was found to be better than that of **8b**. All the polymers were fully characterized using differential scanning calorimetry, thermogravimetric analysis, and gel permeation chromatography analyses. Kinetic studies on the ROP reaction of LA confirmed that the rate of polymerization followed the order $\text{Ba} \gg \text{Sr} \approx \text{Ca}$.



INTRODUCTION

Recently, polylactide (PLA), a biodegradable and biocompatible polymer, has garnered much interest as an excellent replacement for conventional petrochemical materials in a variety of applications, including packaging, fibers, and biomedical devices.^{1–4} PLA is produced from the ring-opening polymerization (ROP) of lactide (LA) monomers derived from renewable resources, which are nontoxic.⁵ PLAs with different microstructures can be synthesized by varying different isomers of the LA monomer, selectivity of initiators, and polymerization conditions. In addition, PLA has unique physical properties that render it useful in a wide range of commodity applications as well as in life sciences.^{6,7} The ROP of racemic lactide (*rac*-LA) may produce either (a) an isotactic PLA or (b) a heterotactic PLA and atactic PLA. Isotactic PLAs obtained from the ROP of *rac*-LA have higher melting points (T_m) and modulus than atactic PLAs. In this context, there is increasing interest in methods that allow for the preparation of isotactic PLAs in a reproducible and controlled fashion.^{8–11}

Hitherto, catalytic ROP of cyclic esters, such as LAs and lactones, has been explored by the use of organocatalysts,^{12–14} as well as discrete metal precursors of chiral ligands, such as complexes of tin,^{15,16} aluminum,^{17–19} zinc,^{20,21} magnesium,^{22,23} iron,^{24,25} titanium,^{26,27} indium,²⁸ yttrium,²⁹ rare-earth metals,^{30,31} and organo-initiators.³² Generally, only a limited number of isoselective achiral catalysts are well-known in the literature (Figure 1),³³ and most isoselective ROPs are based on expensive chiral catalysts. Several highly active achiral catalysts³⁴ are well-known for producing amorphous, heterotactic PLAs of low PDI from *rac*-LA.^{35–44} However, it is highly desirable to develop a new achiral catalyst^{45–47} that can promote stereoselective transformations by adopting chirality in the propagating step by being chain-end bound to the catalyst in a chain-end controlled mechanism. This strategy is

Received: November 8, 2017

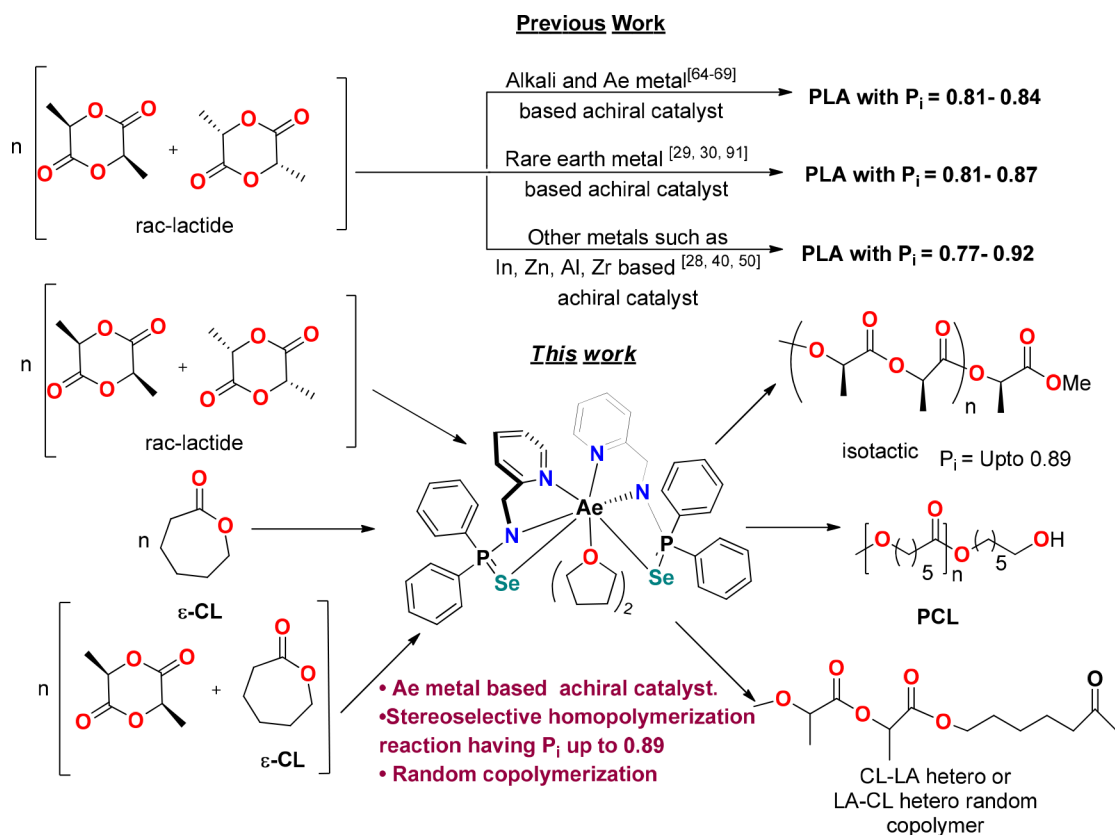


Figure 1. Type of achiral catalysts.

advantageous, as it prevents the need for regenerated chiral precursors that control the stereochemistry in *rac*-LA.^{48–51}

In certain medicinal applications requiring advanced drug-delivery materials with precise control over the polymer degradation rate, the use of homopolymers is often detrimental, due to their rapid biodegradability and impermeability to most drug molecules. It has been shown that the copolymerization of LA with ϵ -caprolactone (ϵ -CL) can lead to variety of biodegradable copolymers with improved properties, when compared to their parent polymers, polycaprolactone (PCL) and PLA homopolymers.^{52,53} PLA obtained from *rac*-LA is typically characterized as brittle, with low strength and short in vivo lifespan (typically a few weeks), whereas PCL is known to be tough, high in mechanical strength, and has a lifespan of about a few years. Therefore, combining these two materials into a random copolymer of varying compositions has been a very useful technique in producing biomaterials tailored for specific applications. The ring-opening copolymerizations of LA and caprolactone (CL) are generally carried out using stannous octoate, zinc alkoxide, aluminum isopropoxide, or titanium isopropoxide as the catalyst.^{54–60} However, due to the relatively high reactivity of LA when compared to CL, this reaction often leads to the formation of copolymers with blocky structures.⁶¹ Yttrium amidate complexes have been shown to produce PCL of high molecular weight.⁶² However, the moisture sensitivity of this catalyst limits its application toward achieving scalable, functionalized polymer synthesis.

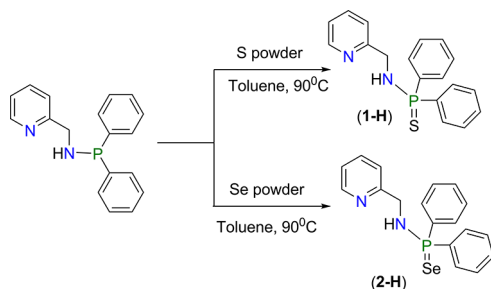
Indeed, there are very few examples of random copolymer formation using designed catalysts, and only a few from titanium and rare-earth metal-based catalysts have been reported.^{63,64} There are even fewer reports of the use of sodium and potassium complexes as precatalysts in the case of

homopolymerization,^{65–69} and the use of nontoxic heavier Ae metal catalysts is much less explored albeit some magnesium complexes are known.^{22,23}

Recently, we employed a series of Ae metal complexes as catalysts in the ROP of *rac*-LA and ϵ -CL at room temperature.⁷⁰ Despite high selectivity toward LA polymerization, these complexes failed to act as suitable catalysts for the copolymerization of *rac*-LA and ϵ -CL. To explore the further activity of Ae metal complexes in more diverse polymerizations, we introduced a series of Ae metal complexes with functionalized P–N ligands for the homopolymerization of *rac*-LA and ϵ -CL, followed by copolymerization of *rac*-LA and ϵ -CL. All the complexes showed high activity, with high isoselectivity, and controlled polymerization at high molecular weights for the ROP of *rac*-LA and ϵ -CL. Most importantly, the Ae metal complexes can be used for copolymer synthesis with short sequence lengths, close to 1:1 monomer incorporation, and good M_n due to transesterification. We intend to further explore our synthesis of random copolymers with these readily modified ligand sets to access a family of polymerization catalysts which will afford a large scope of M_n , with shorter sequence length and increased levels of transesterification.

RESULTS AND DISCUSSION

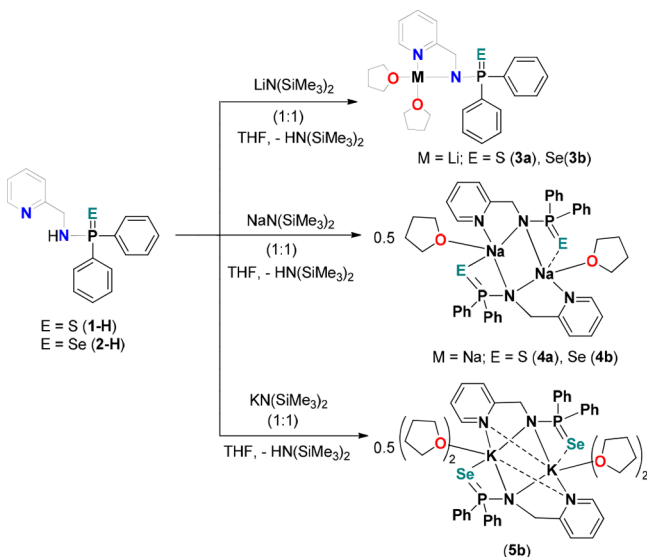
Ligand Synthesis. The ligand precursors, 2-picolyldiamino-diphenylphosphane chalcogenide [(Ph₂P(=E)NH–CH₂–(C₃H₄N)] (E = S (**1-H**); Se (**2-H**)), were readily obtained in excellent yield and high purity by the equimolar oxidation of 2-picolyldiamino-diphenylphosphane using a slight excess of elemental sulfur or selenium in toluene at 90 °C temperature (Scheme 1). The ¹H NMR spectra of both the ligands **1-H** and **2-H** are consistent with their composition. In their ³¹P{¹H}

Scheme 1. Synthesis of protic ligands **1-H** and **2-H**

NMR spectra, similar resonances at $\delta_p = 59.7$ (for **1-H**) and 57.6 ppm (for **2-H**) are consistent with those of related compounds [(Ph₂P(=S)NH-CO(C₅H₄N))] ($\delta_p = 54.4$ ppm) and [(Ph₂P(=Se)NH-CO(C₅H₄N))] ($\delta_p = 47.8$ ppm).⁷¹

The solid-state structure of **1-H** and **2-H** is shown in Figures FS1 and FS2 in Supporting Information. The P–E bond distances [1.9553(7) for **1-H** and 2.1061(7) Å for **2-H**] are in good agreement with those of previously reported compounds [Ph₂P(S)NHCPH₃] [1.9472(7) Å] and [Ph₂P(Se)NH(2,6-Me₂C₆H₃)]^{72–77} [2.1019(8) Å], and thus can be diagnosed as P = S and P = Se double bonds. The P–N bond distance of 1.662(2) Å is consistent with those measured in other phosphinamines.^{72–77}

Alkali Metal Complexes. Alkali metal complexes, with molecular formulas [M(THF)₂(Ph₂P(=E)NCH₂(C₅H₄N))] [M = Li, E = S (**3a**), Se (**3b**)] and [{"M(THF)_n(Ph₂P(=E)NCH₂(C₅H₄N))₂] [M = Na, E = S (**4a**), Se (**4b**); M = K, E = Se (**5b**)], were prepared by the reaction between **1-H** or **2-H** and [MN(SiMe₃)₂] (M = Li, Na, K) in THF (Scheme 2). All five

Scheme 2. Synthesis of Alkali Metal Complexes **3a**, **3b**, **4a**, **4b**, and **5b**

complexes were characterized using spectroscopic and analytical techniques, and the solid-state structures of complexes **3a**, **3b**, **4a**, **4b**, and **5b** were confirmed by single-crystal X-ray diffraction analysis.

The molecular structures of **3a** and **4a** confirm the attachment of the sulfide ligand **1** to lithium and sodium ions respectively, whereas the solid-state structures of **3b**, **4b**, and **5b** reveal the bonding between the selenide ligand **2** and lithium,

sodium, and potassium ions, respectively. The details of the structural parameters are given in Table TS1 in the Supporting Information. Both the lithium complexes are monomeric, whereas the sodium and potassium complexes are dimeric in nature. The solid-state structures of complexes **3a**, **3b**, **4a**, **4b**, and **5b** are shown in Figures FS3, FS4, FS5, FS6, and FS7 in Supporting Information, respectively.

Ae Metal Complexes. Using a known strategy,^{78–80} the one-pot reaction of **2-H** with [KN(SiMe₃)₂] in THF, followed by the addition of AeI₂ (in 2:2:1 molar ratio), yielded the homoleptic complexes [κ^2 -{(Ph₂P(=Se)NCH₂(C₅H₄N))₂Mg(THF)] (**6b**) and [κ^3 -{(Ph₂P(=Se)NCH₂(C₅H₄N))₂M(THF)_n] (M = Ca (**7b**), Sr (**8b**), Ba (**9b**)) in good quantities (Scheme 3). The newly synthesized Ae complexes **6b**, **7b**, **8b**, and **9b** were characterized using spectroscopic and analytical techniques. The solid-state structures of complexes **6b** and **9b** were confirmed by single-crystal X-ray diffraction analysis.

The Ae metal complexes are readily soluble in toluene and THF. A singlet resonance was observed for each complex in the ³¹P{¹H} NMR spectra measured in C₆D₆ at δ_p 70.6 (for **6b**), 71.0 (for **7b**), 70.9 (**8b**), and 70.9 (**9b**) ppm, along with two satellite peaks due to the coupling of P–Se with the adjacent selenium atom. These chemical shift values are significantly shifted toward the lower field compared to that of free ligand **2-H** ($\delta_p = 57.6$ ppm). In the ¹H NMR spectra of each complex, the absence of a resonance signal at 4.03 ppm (assigned for –NH proton of ligand **2-H**) confirms the formation of a monoanionic fragment of ligand **2**. A doublet signal of each complex was observed at δ_H 4.26 (for **6b**), 4.16 (for **7b**), 4.26 (for **8b**), and 4.16 (**9b**) ppm due to the resonance of methylene protons present in the 2-picolylamino-diphenylphosphane selenide ligand backbone.

There is also considerable interest in Ae organometallics, in particular, the non-cyclopentadienyl-based ligand system,^{81–84} and complexes **6b–9b** represent, to the best of our knowledge, the first examples of Ae metal complexes with the 2-picolylamino-diphenylphosphane selenide ligand backbone. Therefore, their molecular structures in the solid state were determined using X-ray diffraction analysis. The crystals of complexes **7b** and **8b** diffract poorly. However, the molecular structures of magnesium complex **6b** and barium complex **9b** were determined using single-crystal diffraction analysis. The details of the structural parameters are given in Table TS1 in the Supporting Information. The solid-state structures of complexes **6b** and **9b** are shown in Figures 2 and 3, respectively. In the magnesium complex **6b**, a κ^2 -coordination mode of the ligand was observed, leaving the selenium atom without any coordination. In addition, a coordinated THF molecule takes the formal coordination number around the magnesium ion to five. Thus, the arrangement around the magnesium ion is an intermediate structure, between a square-based pyramidal and trigonal bipyramidal geometry. However, with a geometric parameter of $\tau_5 = 0.69$,⁸² the metal ion can be best described as having a highly distorted trigonal bipyramidal geometry around it, with N2, N4, and O1 atoms in equatorial positions, and N1 and N3 atoms in axial positions. Two planes—defined by Mg1, N4, C12, C7, N3, and N1, Mg1, N2, C6, C5—are non-coplanar, as indicated by the dihedral angle of 59.8° between them. We noted that in complex **6b**, both the pyridine nitrogen and amido-nitrogen atoms maintain a *trans* arrangement to each other through the magnesium ion.

In the molecular structure of barium complex **9b**, both the ligand fragments exhibited the κ^3 coordination mode using

Scheme 3. Synthesis of Ae Metal Complexes (6b–9b)

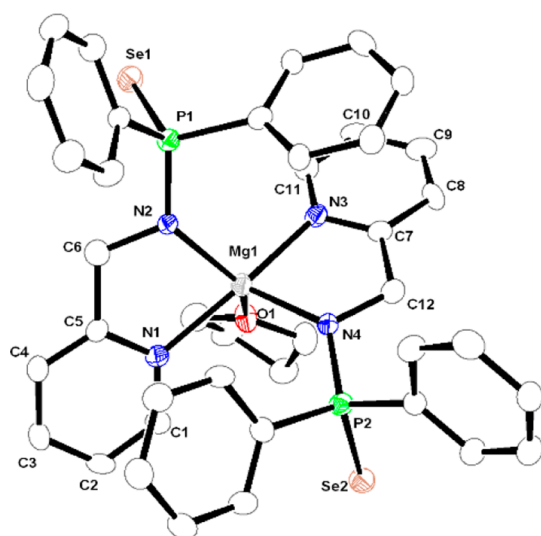
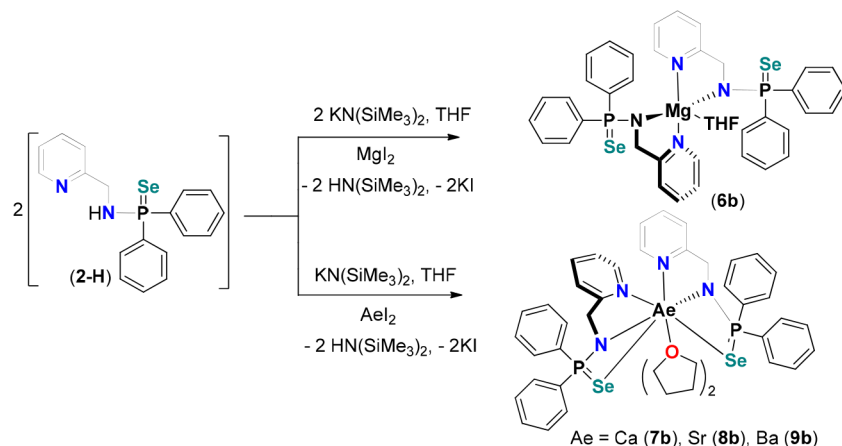


Figure 2. Molecular solid-state structure of $[\kappa^2\text{-(Ph}_2\text{P(=Se)NCH}_2\text{-(C}_5\text{H}_4\text{N)Mg(THF)}]$ (**6b**). Selected bond lengths (Å) and angles (deg) are Mg1–N1 2.159(5), Mg1–N2 2.076(5), Mg1–N3 2.143(5), Mg1–N4 2.056(5), Mg1–O1 2.107(5), P1–Se1 2.1377(17), P2–Se2 2.1397(18), N1–Mg1–N2 79.4(2), N1–Mg1–N3 163.7(2), N1–Mg1–N4 110.6(2), N2–Mg1–N3 105.0(2), N2–Mg1–N4 122.0(2), N3–Mg1–N4 80.7(2), N1–Mg1–O1 82.9(2), N2–Mg1–O1 130.1(2), N3–Mg1–O1 82.4(2), N4–Mg1–O1 107.9(2).

pyridyl, amido nitrogen, and selenium atoms to coordinate with the barium ion. The barium center is 8-fold coordinated, owing to ligation from the additional two THF molecules. Thus, the barium ion can be best described as having a distorted square antiprismatic geometry around it. Each ligand fragment formed one five-membered (Ba1–N1–C5–C6–N2 or Ba1–N3–C23–C24–N4) and one four-membered (Ba1–N2–P1–Se1 or Ba1–N4–P2–Se2) metallacycle, fused together in the metal coordination polyhedron. We noted that in complex **9b**, both ligands were bonded to the metal ion in a *cis*-orientation, unlike the magnesium complex **6b**. The Ba–Se distances [3.4185(1) and 3.4161(1) Å] are consistent with those in the complex we have previously reported [$[\{\text{Ph}_2\text{P(Se)N}\}_2\text{C}_6\text{H}_4\text{]Ba(THF)}_3$ (3.4706(9) and 3.4071(9) Å)].

ROP of *rac*-LA. All the complexes (**6b–9b**) were tested as catalysts for the ROP reaction of *rac*-LA and values are shown in Table 1. In the case of magnesium complex **6b** the rate of polymerization is very slow, and only 47% conversion was

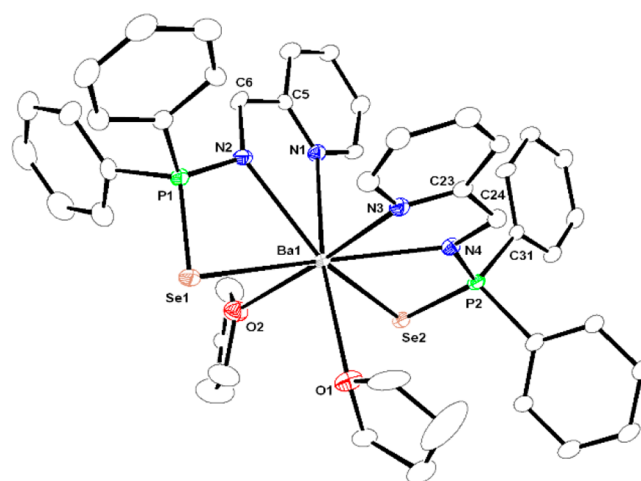


Figure 3. Molecular solid-state structure of $[\kappa^3\text{-}\{(\text{Ph}_2\text{P(=Se)NCH}_2\text{-(C}_5\text{H}_4\text{N)}\}_2\text{Ba(THF)}_2]$ (**9b**). Selected bond lengths (Å) and angles (deg) are Ba1–N1 2.858(8), Ba1–N2 2.740(8), Ba1–Se1 3.4185(11), Ba1–N3 2.875(7), Ba1–N4 2.760(7), Ba1–Se2 3.4161(12), Ba1–O1 2.825(7), Ba1–O2 2.789(7), N1–Ba1–N2 58.4(2), N1–Ba1–Se1 116.17(15), N1–Ba1–N3 99.0(2), N1–Ba1–N4 82.5(2), N1–Ba1–Se2 88.66(16), N2–Ba1–Se1 58.45(14), N3–Ba1–N4 58.0(2), N3–Ba1–Se2 114.41(15), N4–Ba1–Se2 58.85(15), O1–Ba1–O2 94.1(2), N2–P1–Se1 109.1(3), S1–Ba1–Se2 147.20(3).

achieved after 24 h (Figure FS60 in Supporting Information). So further polymerization reactions were carried out using other alkaline earth metal catalysts. The polymerization of *rac*-LA, catalyzed by complexes **7b** and **8b**, was accomplished with 99% conversion within 30 min [100:1 ratio of [*rac*-LA]:[**7b**]/[*rac*-LA]:[**8b**] in toluene (Table 1, entries 1 and 6), [Cat.] = 1.0 mM, room temperature]. In contrast, when the corresponding barium complex **9b** was used as the catalyst, the reaction was much faster, and 99% conversion was achieved in 5 min (Table 1, entry 11). However, the same reaction, using **9b** as the catalyst, took 3 h to achieve 50% monomer conversion when THF was used as solvent and 25% when CHCl₃ was used (Table 1, entries 17 and 18). The varying reaction rates can be ascribed to the competitive coordination of THF and different solvent polarities with active metal centers, which diminish the LA–metal interaction. We have observed and reported similar phenomena previously.⁶⁹ Therefore, toluene was chosen as an optimized solvent to eliminate solvent influence in the ROP of LA. When we

Table 1. Polymerization of *rac*-LA in the Presence of Alkaline Earth Metal Complexes Bearing Phosphinamine Selenide Ligand (7b–9b)^a

entry	catalyst	M:1	solvent	time (h:m)	conversion ^b	$M_{n,theo}$ (kDa)	$M_{n,exp}$ ^c GPC (kDa)	PDI	P_i ^d
1	7b	100	toluene	00.30	99	14.3	15.9	1.24	0.89
2	7b	200	toluene	00.30	99	28.5	29.9	1.23	0.87
3	7b	300	toluene	00.35	95	41.1	42.3	1.27	0.85
4	7b	400	toluene	00.40	97	55.9	57	1.04	0.83
5	7b	500	toluene	01.00	99	71.3	74.1	1.64	0.85
6	8b	100	toluene	00.30	99	14.3	15.9	1.35	0.79
7	8b	200	toluene	00.30	97	28.5	29.9	1.57	0.77
8	8b	300	toluene	00.30	99	41.1	40.6	1.38	0.76
9	8b	400	toluene	00.35	99	54.7	54.9	1.50	0.75
10	8b	500	toluene	00.40	95	69.8	68.2	1.12	0.71
11	9b	100	toluene	00.05	99	14.3	14.6	1.35	0.70
12	9b	200	toluene	00.05	99	28.5	29.5	1.31	0.58
13	9b	300	toluene	00.05	99	42.8	45.9	1.40	0.65
14	9b	400	toluene	00.06	99	57.1	55.8	1.52	0.62
15	9b	500	toluene	00.08	99	71.3	73.9	1.01	0.60
16	9b	1000	toluene	00.10	91	131.04	125.4	1.51	0.61
17	9b	100	THF	03.00	50	7.2	5.6	1.35	0.55
18	9b	200	DCM	03.00	25	3.6	2.4	1.75	0.55
19	7b	200	toluene	00.30	99	28.5	27.5	1.23	0.86
20	7b	300	toluene	00.30	99	41.1	42.9	1.24	0.86 ^e

^aIn toluene at 25 °C, [catalyst] = 1 mM. ^bConversions were determined by ¹H NMR spectroscopy. $M_{n,theo}$ = molecular weight of chain-end + 144 g mol⁻¹ × (M:1) × conversion. ^cIn THF (2 mg mL⁻¹) and molecular weights were determined by GPC-LLS (flow rate = 0.5 mL min⁻¹). Universal calibration was carried out with polystyrene standards, laser light scattering detector data, and concentration detector. Each experiment was duplicated to ensure precision. ^dCalculated according to Method A, using the relative integrals of rmr and rmm resonance. ^eThe polymerization was carried out in the presence of benzyl alcohol in a monomer: catalyst: BnOH ratio of 300:1:10.

increased the quantity of monomer, up to 1000 equiv of *rac*-LA with **9b** as the catalyst in toluene, the polymerization was completed in less than 10 min, affording the desirable high molecular weight of 125 kg/mol, with an acceptable polydispersity index (PDI) of 1.51, as well as a good P_i value of 0.61 at room temperature (Table 1, entry 16). These results clearly indicate that Ae metal complexes are very effective catalysts for the synthesis of PLAs with high molecular weight epimerization.^{85–87}

Despite the high overall rates of polymerization, molecular weights of the polymers (M_n) agree well with their calculated values, and increase in linear fashion with an increase in the quantity of the monomer (Table 1, entries 1–5 and Figure 4), retaining the narrow molecular weight distributions. A second set of feed experiments, carried out using the same catalyst, confirmed that the molecular weights of polymers are under control (Figure 4). Compared to the barium complex **9b**, the calcium and strontium complexes, **7b** and **8b** respectively, are slightly less active (Table 1, entries 1–15), which suggests that the metal ion plays a vital role in the initiation step for the activation of the monomer species.

The catalysts in this family are isoselective. The P_i values can be calculated by substituting integrations of tetrad sequences, from ¹H{¹H} NMR spectroscopy.⁸⁸ The tacticity of PLA is calculated using a set of equations derived from a Bernoullian statistical model.⁸⁸ In the case of the calcium complex **7b**, isoselectivities of $P_i = 0.89, 0.87,$ and 0.85 were achieved when the stoichiometric ratios of [LA]:[**7b**] were varied in the order of 100:1, 200:1, and 300:1, respectively, in toluene at room

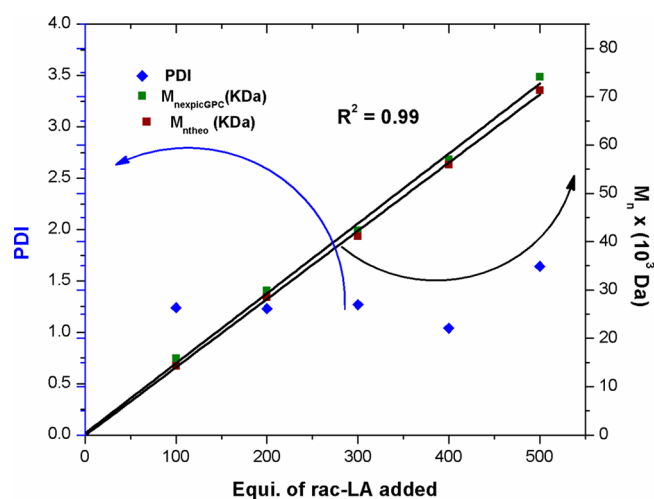


Figure 4. Plot of observed PLA $M_{n,theo}$ and $M_{n,exp}$ (■) with molecular weight distribution (PDI) (blue diamonds) as functions of LA:**8b** in (25 °C, Tol, 99% conv.) The line indicates calculated M_n values based on the LA:**8b** ratio.

temperature (Table 1, entries 1–3) (Figures FS72–FS75 in Supporting Information). To the best of our knowledge, this is the highest P_i value obtained so far by an Ae catalysts.⁷⁰ Even increasing the quantity of *rac*-LA to 500:1 did not perturb the degree of isoselectivity ($P_i = 0.85$) (Table 1, entry 5), which clearly indicates the controlled manner of polymerization. The enhancement of isoselectivity may be attributed to the

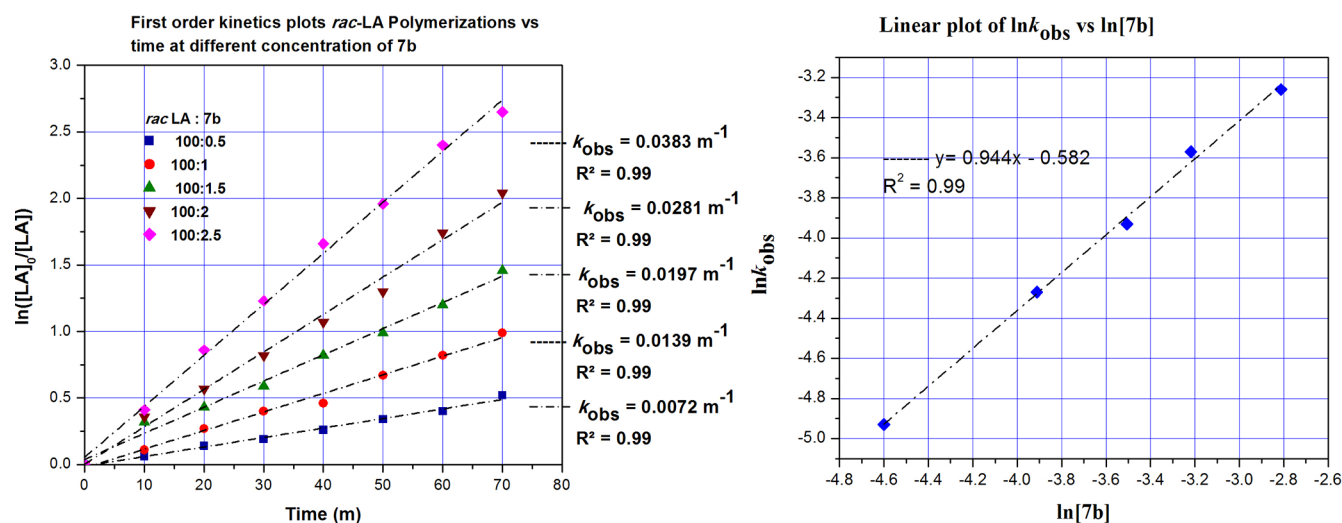


Figure 5. (Left) Kinetics plots of the *rac*-LA versus time in toluene at 25 °C with different concentration of catalyst **7b** as an catalyst. $[7b]_0 = 0.5, 1.0, 1.5, 2.0, \text{ and } 2.5 \text{ mM}$; $[rac\text{-LA}]_0 = 2 \text{ M}$. (Right) Plots of $\ln k_{obs}$ versus $\ln [7b]_0$ for the polymerization of *rac*-LA with catalyst **7b** as an catalyst in toluene at 25 °C. $[rac\text{-LA}]_0 = 2 \text{ M}$.

increased interaction between the lactide and the active metal site of the catalyst. The high isoselectivities are also maintained with increase in temperature, as observed from the P_i values, which were quite unchanged (Table 1, entry 19, $P_i = 0.86$ for **7b**). In addition, a high T_m of 186 °C of the polymer (Figure FS84 in Supporting Information), which is significantly higher than that of the optically pure poly(L-LA), is in good agreement with the highly isotactic polymer structure.⁸⁹ Additionally, the PLAs obtained from catalyst **7b** are stable up to 280 °C, as shown on the TGA curve (Figures FS81–FS83 in Supporting Information), which indicates a very high level of polymer purity. When complex **8b** was used, similar isoselectivities were achieved for the ROP of *rac*-LA (Table 1, entries 6–10) (Figures FS72–FS75 in Supporting Information), but with respect to **7b**, the degree of isoselectivity decreased slightly ($P_i = 0.79\text{--}0.71$) (Figures FS72–FS75 in Supporting Information), due to the increase in size of active metal center from **7b** to **8b**, which provides a more open coordination geometry to the metal ion, whereas isoselectivity is induced due to the steric congestion around the metal center as we move toward the smaller Ae metals. Subsequently, in case of complex **9b**, the degree of isoselectivity dropped significantly, to 0.58 (Figure FS77 in Supporting Information). This is quite expected, as a gradual decrease in stereo control on decreasing steric shielding is typical, and well-reported in the literature.^{70,90}

A comparison of the selectivities listed in Table 1 using the Bernoullian statistical model shows that a decrease in metal steric hindrance correlates to increased P_i values, while increasing the steric bulk of the ligands does not result in an appreciable increase in P_i values above 0.71. ¹H NMR spectra revealed the end-group analysis of the polymer chains, which were capped at one end by one benzyl ester and at the other by one hydroxyl group (Figure FS69 in Supporting Information).

Kinetic experiments were performed with $[rac\text{-LA}]_0/[Ae]_0$ ratios ranging from 100 to 500. In each case, *rac*-LA (0.228 g, 2.0 mmol) was added to a solution of each catalyst (**7b**–**9b**) (0.01, 0.02, 0.03, 0.04, 0.05 M respectively) in $CDCl_3$ (1 mL), at room temperature. The solution was kept in the NMR tube at 25 °C, and at the indicated time intervals, the tube was analyzed by ¹H NMR. As expected, plots of $[LA]_0/[LA]$ versus

time for a wide range of $\ln\{[Ph_2P(Se)NCH_2C_6H_4N]_2Ca(THF)_2\}$ are linear, clearly showing first-order dependence on $[rac\text{-LA}]$ for all the ratios (Figure 5). Thus, the rate expression can be summarized as follows:

$$-d[LA]/dt = k_{app}[LA]^1$$

$$\{[Ph_2P(Se)NCH_2C_6H_4N]_2Ca(THF)_2\}^x = k_{obs}[LA]^1$$

$$\text{where } k_{obs} = k_{app}$$

$$\{[Ph_2P(Se)NCH_2C_6H_4N]_2Ca(THF)_2\}^x$$

Furthermore, a double-logarithm plot (Figure 5) of the observed rate constants (k_{obs}), obtained from the slopes of the best fit lines to the plots of $\ln([rac\text{-LA}]_0/[rac\text{-LA}]_t)$ versus time as a function of $\ln [7b]_0$ was fit to a straight line propagation is also first-order with catalyst concentration, indicating that the *rac*-LA polymerization follows the monometallic, intramolecular coordination–insertion mechanism ($R^2 = 0.999$) with a slope of 0.944. Similar observations were made about other catalysts **8b** and **9b** (Figures FS41–FS49 in Supporting Information).^{91–94} Therefore, the overall rate equation for the ROP of *rac*-LA, in the presence of a catalyst, follows second-order dependence, and may be represented as

$$\text{rate} = -d[LA]/dt = k_p[\text{catalyst}]^1[LA]^1$$

Table 2 represents a comparative study of the rate constants for the ROP of *rac*-LA in the presence of catalysts **7b**–**9b**, which shows that k_{obs} values gradually increase from 0.0139 $M^{-1} m^{-1}$ to 0.029 $M^{-1} m^{-1}$ for **7b** and **8b** respectively, whereas the k_{obs} value of 0.036 ($M^{-1} m^{-1}$) for **9b** is relatively higher. (*rac*-LA:catalyst = 100:1). On the basis of our previous study, the enhanced k_{obs} value of the barium complex could be due to its larger ionic radius, compared to other Ae metal ions,⁷⁰ which enhances the availability of free space around the metal center, favoring catalyst–LA interactions, which eventually enhances the ROP of *rac*-LA. Notably, the calcium and strontium (**7b** and **8b** respectively) complexes have nearly similar rates, within error, due to the smaller difference of ion size between them.

Table 2. Comparison of Rate Constants for Polymerization of *rac*-LA with Various Concentrations of **7b**, **8b**, and **9b** as Catalyst

s. no.	catalyst	<i>rac</i> -LA: catalyst	k_{obs} in (M ⁻¹)
1	7b	100:0.5	0.0072
2	8b	100:0.5	0.0201
3	9b	100:0.5	0.0256
4	7b	100:1	0.0139
5	8b	100:1	0.029
6	9b	100:1	0.036
7	7b	100:1.5	0.0197
8	8b	100:1.5	0.039
9	9b	100:1.5	0.051
10	7b	100:2	0.0281
11	8b	100:2	0.0489
12	9b	100:2	0.069
13	7b	100:2.5	0.0383
14	8b	100:2.5	0.0575
15	9b	100:2.5	0.092

Activation Parameters for the ROP of *rac*-LA. Finally, we also investigated the effect of temperature on the rate of ROP of *rac*-LA using catalysts **7b–9b**. From Figure 6, it is clear that the polymerization rate increased with increase in temperature. From the five k_{obs} values determined at different temperatures, the activation energy of the polymerization reaction using catalysts **7b–9b** was deduced, by fitting $\ln k_{\text{obs}}$ vs T^{-1} according to the Arrhenius equation (Figure 6). The activation energy, E_a , for *rac*-LA polymerization using **7b** was 23.84(3) kJ mol⁻¹. The activation energies for **7b** and **8b** are comparable, but they were much lower than that calculated when **9b** was used (Figures FS51–FS59 and Tables TS12–TS16 in Supporting Information).^{95,96}

The other activation parameters for the ROP of *rac*-LA catalyzed by **7b–9b** in CDCl₃ were found to be ΔH^\ddagger 25.87(4) kJ/mol, ΔS^\ddagger -195.9 (7) J/(mol K), ΔH^\ddagger 20.49 (3) kJ/mol, ΔS^\ddagger -192.1(1) J/(mol K), ΔH^\ddagger 22.66(4) kJ/mol, and ΔS^\ddagger -200.84 (3) respectively (Figures FS51–FS59 and Tables TS12–TS16 in Supporting Information). These values were calculated from the temperature-dependent second-order rate

constants determined from k_{obs} values divided by temperature values, as provided in Table TS16 in Supporting Information. The Eyring plot (Figure 6, right) indicates similar ordered transition states in a coordination–insertion mechanism.^{89–92} ΔG^\ddagger values were calculated for the ROP of *rac*-LA catalyzed at 25 °C (Table TS16 in Supporting Information).⁹⁷

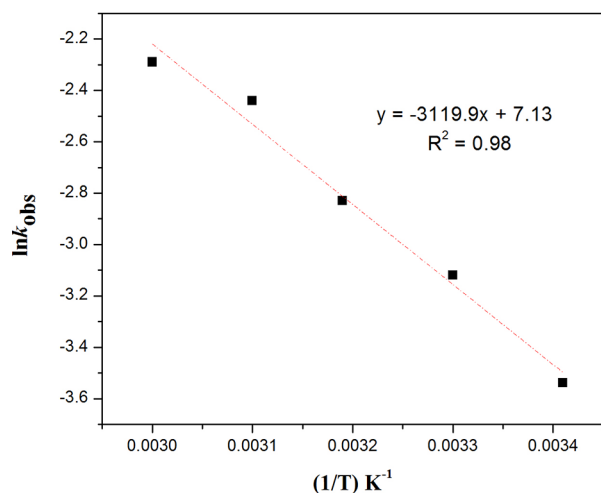
In order to understand the mechanism and effect of the external initiator of the polymerization reaction, we conducted a typical kinetic study for the ROP reaction of *rac*-LA in the presence of an alcohol. This helped us determine the reaction order with respect to the lactide, catalysts **7b–9b**, and benzyl alcohol (BnOH), as well as establishing the pathway of the ROP mechanism. The results indicated that the reaction rate exhibits first-order dependence with respect to *rac*-LA and catalysts **7b–9b**, whereas it follows zero-order dependence with respect to BnOH (Figures FS65 and FS66 in Supporting Information). At various concentrations of complex **9b** (0.01, 0.02, 0.03, 0.04, 0.05 mM) and concentrations of [*rac*-LA]₀ and [BnOH]₀ fixed at 2 M and 1.0 mM respectively, the k_{obs} values were found to be identical to those obtained in the absence of BnOH. In addition, when the concentrations of BnOH (0.02–0.2 M) were varied, but the concentration of **9b** (0.02 M) and *rac*-LA (0.228 g, 2.0 mmol) were kept constant, the k_{obs} values remained unchanged. Thus, the lack of dependence on the concentration of BnOH confirms its zero-order contribution to the rate law. The overall rate may be expressed as follows:

$$-d[\text{LA}]/dt = k_2[\text{LA}]^1[\mathbf{9b}]^1[\text{BnOH}]^0$$

On the basis of the information set out above, the mechanism is shown in Scheme 4.

In the first step, the phosphorus–selenide double bond (P=Se) of the catalyst is converted into a single bond to form a zwitterionic species, which initiates the polymerization reaction in the presence of one molecule of *rac*-LA (Scheme 4). The metal–LA interaction in the initiation step is directly proportional to the size of the metal. The greater the size of the metal, greater is the possibility of the metal–lactide interaction period.⁹¹ The steric crowding enhances the initiation of the selenide to a monomer, by releasing the

Arrhenius plot of $\ln k_{\text{obs}}$ vs $(1/T)$ for ROP of *rac*-LA catalyzed by **9b**



Eyring plot for **9b**

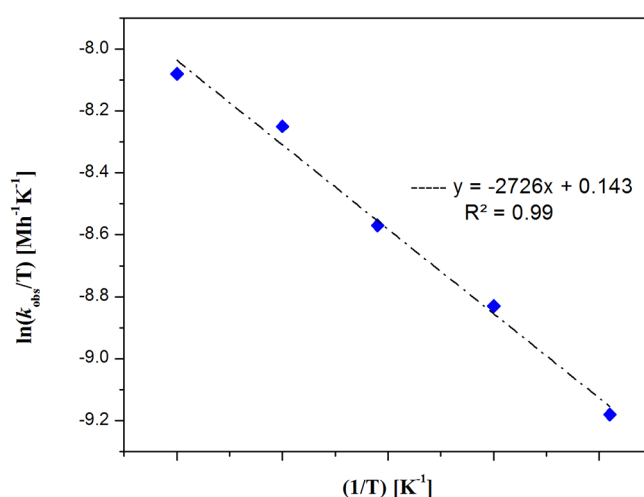
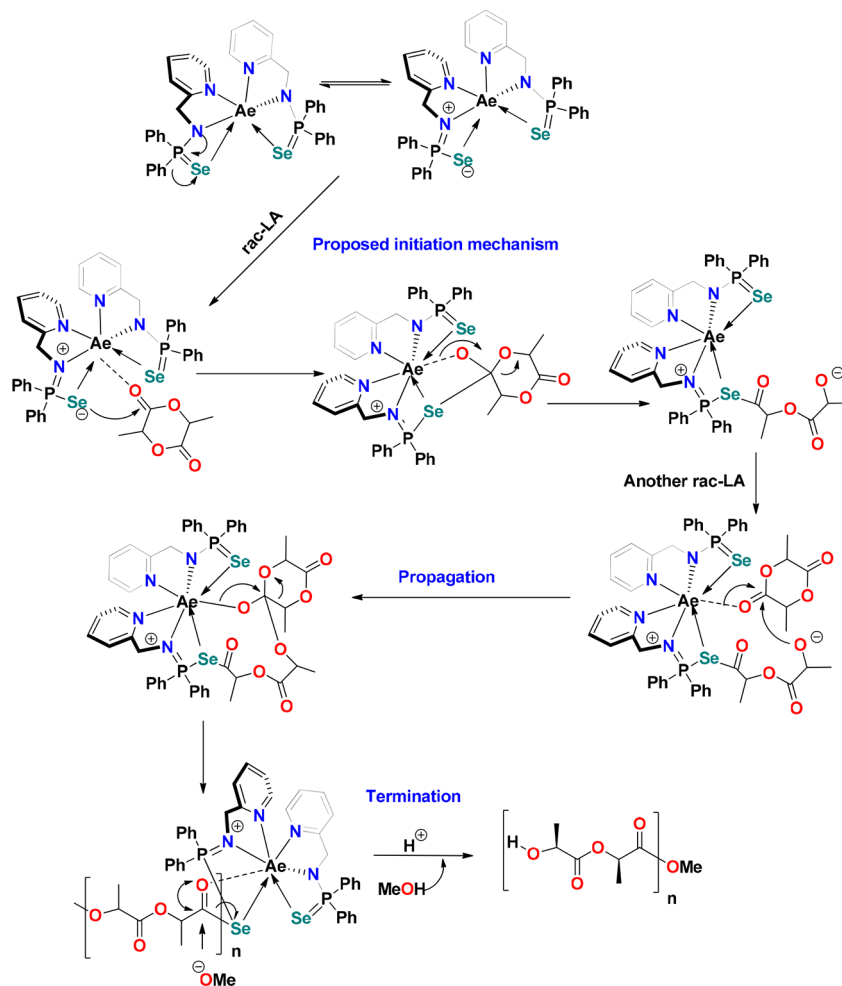


Figure 6. Arrhenius plot (left) of $\ln(k_{\text{obs}})$ versus $(1/T)$ and Eyring plot (right) of $\ln(k_{\text{obs}}/T)$ versus $(1/T)$ for catalyst **9b** for the polymerization of *rac*-LA (0.01 M) with [LA] = 2.0 M in CDCl₃ having E_a = 25.93 (5) kJ mol⁻¹, ΔH^\ddagger = 22.66(4) kJ mol⁻¹, ΔS^\ddagger = -200.84 (3) J mol⁻¹ K⁻¹ (CDCl₃).

Scheme 4. Proposed Mechanism for *rac*-LA Polymerization Initiated by Catalyst 7b–9b

unstable energy of repulsion. We have already established similar results in our work, as reported previously.⁷⁰

In addition, we carried out reactions by loading the monomer and catalyst in the ratios of 5:1 and 10:1, and analyzed the reaction mixture using ¹H NMR, ³¹P, and ¹³C spectra to prove the mechanism pathway. The ¹H NMR spectra clearly indicated the end group of the polymer, and that the catalyst is bound to the polymer in the expected ratio (Figure FS64 in Supporting Information). We also observed two sharp resonance peaks in the ³¹P{¹H} NMR spectra, at δ 71.9 and 57.6 ppm for **9b** (Figure FS67 in Supporting Information), which indicated the chemically nonequivalent nature of the two phosphorus atoms during the polymerization process.

ROP of ϵ -CL. The ROP of ϵ -CL was carried out using all the Ae metal complexes (**7b–9b**) as catalysts. A catalyst loading of 0.05 mol % in toluene was used as the catalyst (Table TS21 in Supporting Information) for the ROP of ϵ -CL. As shown in entries 1–10 of Table TS21 in Supporting Information, 99% conversion of the monomer to PCL was achieved within 1 min when complexes **7b** and **8b** were used, whereas almost instant polymerization occurred in the case of complex **9b**. In addition, all the catalysts showed greater control of polymer molecular weight at levels comparable with $M_n(\text{calcd})$, $M_n(\text{GPC})$, and narrow PDIs. We then increased the quantity of the monomer, which showed that the polymerization, up to 1000 equiv of ϵ -CL using complex **9b**, was completed in less than 5 min in toluene at room temperature, affording the desirable high

molecular weight of 110 kg/mol, and an acceptable PDI of 1.27. Due to the larger ionic radius of the barium atom, relative to the calcium and strontium atoms, complex **9b** showed the highest reactivity toward the ROP of ϵ -CL, similar to what was observed in previously reported studies using other barium complexes.^{70,78–80} According to the literature,^{78–80} a possible mechanism is proposed in Supporting Information which is similar to the mechanism proposed for ring opening polymerization of *rac*-LA. The Ae metal complexes, as precatalysts, were extremely fast catalysts, enabling almost complete conversion of 1000 equiv of ϵ -CL in less than 30 s (Table TS21 in Supporting Information). Therefore, no further kinetic studies were undertaken for the polymerization reactions of ϵ -CL.

Copolymerization of *rac*-LA and ϵ -CL. Achieving high conversion of both the monomers as well as controlling their sequence in random distribution have been the key objectives of the developments dedicated toward the ring-opening copolymerization of *rac*-LA and ϵ -CL. Usually, the considerable difference in reactivity between LA and CL in these reactions tends to generate block-domain microstructures. Therefore, random copolymers, with 1:1 incorporation of both monomers, are rare.^{63,64} The catalytic activity of complexes **7b**, **8b**, and **9b** in the ring opening copolymerization of *rac*-LA and ϵ -CL were examined in terms of conversion and average block length with respect to each monomer. Both the barium and strontium complexes showed good activity for the synthesis of copolymers, with the activity of the barium complex (**9b**)

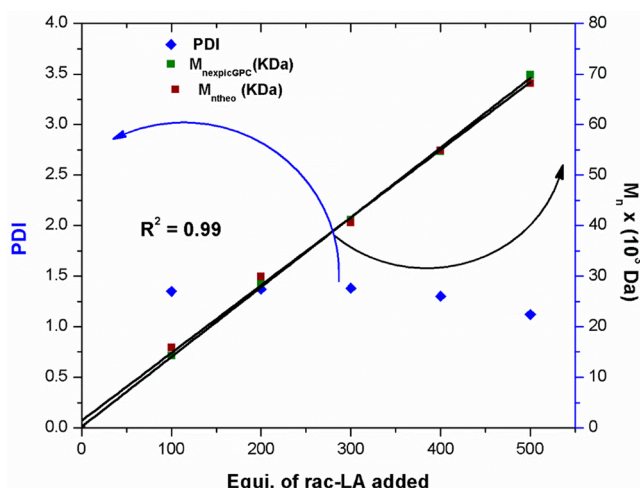


Figure 7. Plot of observed PLA $M_{n,theo}$ and $M_{n,expi}$ (■) with molecular weight distribution (PDI) (blue diamonds) as functions of ϵ -CL: **8b** in (25 °C, Tol, 99% conv.). The line indicates calculated M_n values based on the ϵ -CL:**8b** ratio.

being comparatively higher than that of the strontium complex (**8b**), providing polymers with monomodal molecular weight distributions [PDI(1) = 1.47; PDI(2) = 1.38]. In the case of the calcium complex (**7b**), however, only homo-polymerization products were formed. In the case of the barium complex (**9b**), the incorporation of LA and CL was in the ratio 1:0.18 (85:15) during the first 30 min accounting for a relatively higher reactivity of LA compared to CL. Upon continuing the reaction for an additional 2 h, this ratio was found to improve dramatically to 0.72:1 (42:58), indicating further incorporation of CL monomers. We also observed moderate levels of CL and LA incorporation, when the strontium complex (**8b**) was used, without the need for an excess CL feed. The ^{13}C NMR studies of the copolymer samples obtained at different intervals revealed the average sequence lengths of caproyl (LCL) and lactidyl (LLA) to be 1.8 and 3.6 after one-and-a-half hours, indicating that LA forms a relatively longer chain of PLA with CL reacting modestly (Table 3, entry 2). However, as the reaction proceeded further, their values improved significantly to 1.9 and 2.7 after 2 h, indicating the formation of practically random copolymers (an ideal random copolymer will have LCL = LLA = 2).^{98,99} The ^1H NMR analysis of the copolymer samples obtained after quenching with methanol showed the presence of methyl ester peaks resulting from transesterification, which is considered to lead the randomization of microstructures during copolymer formation. The thermal properties of the copolymers were analyzed using the differential scanning calorimetry (DSC) curve, which showed

that copolymers were amorphous in nature and displayed T_g of -3.3 °C, [T_g (PCL) = -60 °C, T_g (PLA) = 57 °C], (Figure FS99 in Supporting Information). The thermal behavior exhibited in the DSC studies supports a structure that is very close to a random distribution of the two monomers along the polymer chain.

CONCLUSION

In this paper, we have demonstrated the synthesis and structural study of a series of alkali metal and Ae metal complexes supported by 2-picolylamino-diphenylphosphane sulfide and selenide ligands. In the lighter Ae metal magnesium, the selenide ligand behaves in bidentate fashion, leaving both the selenium atoms uncoordinated. However, in the barium complex **9b**, the selenide ligand exhibits tridentate binding mode with the metal ion. The heavier Ae metal complexes **7b**, **8b**, and **9b** were utilized for the ROP of *rac*-LA at room temperature. Although the ROP reaction is fastest for complex **9b**, the highest isoselectivity of PLA ($P_i = 0.89$) was observed for the calcium complex **7b**, due to the smaller ionic radius of calcium. A complete kinetic study of the ROP reaction indicated first-order reaction kinetics with respect to the *rac*-LA and catalyst concentration. The addition of benzyl alcohol did not affect the order of the reaction, indicating that Ae catalysts initiate the ROP of LA in the first step. The Ae metal catalysts **7b–9b** are also active for the ROP of ϵ -CL to yield polycaprolactone, with a narrow PDI. The strontium and barium complexes **8b** and **9b** were used for copolymerization of *rac*-LA and ϵ -CL at room temperature to afford random copolymers in high yield. The random copolymer formation using complex **9b** was evidenced by the average lengths of the caproyl and lactidyl sequences (LCL = 1.9 and LLA = 2.7) of the copolymer, which were formed from a starting feed composition of CL/LA in the ratio of 1:1. With the success of being able to perform both homo-polymerization and copolymerization using a single complex **9b** in an efficient and controlled manner, this system can be extended to the generation of a variety of biodegradable polymers with very good control over the polymer properties. Thus, the present study could lead to a single platform of Ae metal complexes, resulting in a wide range of biodegradable polymers with high yield and selectivity.

EXPERIMENTAL SECTION

General methods. All manipulations involving air- and moisture-sensitive organometallic compounds were carried out under argon using the standard Schlenk technique or argon-filled glovebox. Hydrocarbon solvents (*n*-pentane, toluene) were distilled under nitrogen from LiAlH_4 and stored in the glovebox. THF was dried and deoxygenated by distillation over sodium benzophenone under argon and then distilled and dried over CaH_2 prior to storing in the

Table 3. Copolymerization of ϵ -CL and *rac*-LA Using Catalyst **9b**^a

catalyst	yield ^b	time (h:m)	CL/LA (mol %) ^c	LCL/LLA ^d	$M_{n,theo}$ (KDa)	$M_{n,theo}$ (KDa)	PDI
9b	89	00.30	15/85		27.9	27.5	1.52
9b	87	01.30	28/72	1.8/3.6	27.1	26.3	1.47
9b	85	02.00	36/64	1.9/2.7	26.7	29.9	1.37
9b	83	02.30	49/51		25.9	26.7	1.45
9b	82	03.30	58/42		27.6	28.5	1.38

^aRandom copolymerization conditions: 70 °C, 6 h, [monomer]/[Ae] = 400, 0.200 g (1.38 mmol) LA, 0.33 mL (2.63 mmol) CL. M_n and PDI values for all copolymers were determined from the GPC analysis. ^bIsolated yield. ^cRatio of CL/LA was measured from ^1H NMR. ^dAverage CL and LA chain length determined by ^{13}C NMR. ^eValues obtained by GPC analysis. $M_{n,theo} = ([\text{CL}]/[\text{Ae}] * \% \text{CL} * 114.14) + ([\text{LA}]/[\text{Ae}] * \% \text{LA} * 144.13)$.

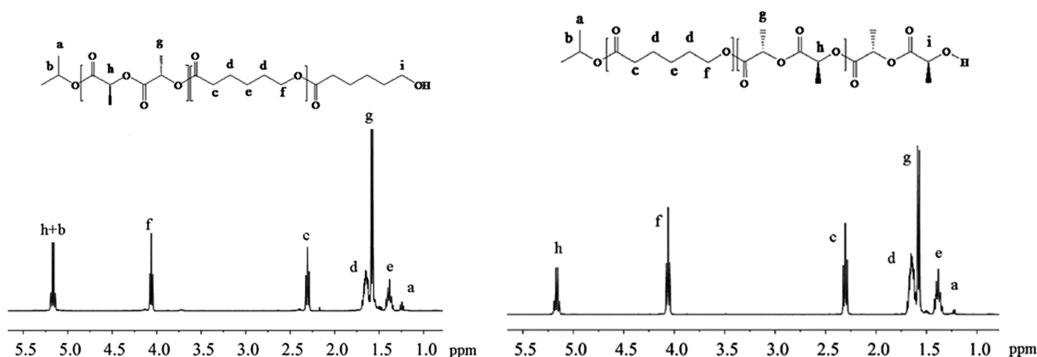


Figure 8. ^1H NMR spectrum of PCL-*co*-PLA and PLA-*co*-PCL copolymer by catalyst **9b** (Table 3, entry 1).

glovebox. C_6D_6 was dried over Na/K, distilled and stored in the glovebox. ^1H NMR (400 MHz), $^{13}\text{C}\{^1\text{H}\}$ NMR (100 MHz), and $^{31}\text{P}\{^1\text{H}\}$ (161.9 MHz) spectra were measured on a BRUKER AVANCE III-400 spectrometer. Elemental analyses were performed on a BRUKER EURO EA at the Indian Institute of Technology Hyderabad. $[\text{Li}\{\text{N}(\text{SiMe}_3)_2\}]$, $[\text{Na}\{\text{N}(\text{SiMe}_3)_2\}]$, $[\text{K}\{\text{N}(\text{SiMe}_3)_2\}]$, MgI_2 , CDCl_3 , *rac*-LA, *ε*-CL were purchased from Sigma Aldrich India.

Preparation of $[(\text{Ph}_2\text{P}(\text{=E})\text{NHCH}_2(\text{C}_5\text{H}_4\text{N}))]$ [E = S (1-H); Se (2-H)]. In a 100 mL Schlenk flask, 1 equiv of (1.2 mL, 11.4 mmol) of 2-(aminomethyl)pyridine, 1 equiv of triethylamine (1.56 mL, 11.4 mmol), and 1 equiv of chlorodiphenylphosphine (2 mL, 11.4 mmol) were mixed together with 40 mL of toluene, and the reaction mixture was stirred for another 6 h. After that, 1.2 equiv of elemental sulfur or selenium powder was added onto it, and the mixture was kept under stirring for another 8 h at 90 °C. Unreacted excess sulfur/selenium was filtered off through a G4 frit, and the filtrate was collected. After evaporation of the solvent from filtrate in vacuo, a colorless solid residue was obtained. The colorless residue was further purified by washing with *n*-pentane or *n*-hexane.

1-H; Yield: 3.2 g (90%). ^1H NMR (400 MHz, CDCl_3): δ 8.38 (1H, ArH), 7.95–7.88 (m, 4H, ArH), 7.49–7.48 (m, 1H, ArH), 7.33–7.31 (m, 6H, ArH), 7.11–7.03 (m, 2H, ArH), 4.17 (dd, J = 8.0 Hz, 2H) 4.07 (s, 1H, NH) ppm. $^{13}\text{C}\{^1\text{H}\}$ NMR (100 MHz, CDCl_3): δ 156.8 (ArC), 156.7 (ArC), 136.2 (ArC), 134.1 (ArC), 133.2 (ArC), 131.8 (ArC), 128.5 (ArC), 122.3 (ArC), 46.3 (CH₂) ppm. $^{31}\text{P}\{^1\text{H}\}$ NMR (161.9 MHz, CDCl_3): δ 59.7 ppm. ($\text{C}_{18}\text{H}_{17}\text{N}_2\text{PS}$) (324.36), calcd C 66.65, H 5.28, N 8.64; found, C 66.31, H 5.09, N 8.49.

2-H; Yield: 4.1 g (97%). ^1H NMR (400 MHz, CDCl_3): δ 8.40–8.38 (dd, J = 3.9 Hz 1H, ArH), 7.95–7.89 (m, 4H, ArH), 7.52–7.48 (m, 1H, ArH), 7.39–7.30 (m, 6H, ArH), 7.13–7.04 (m, 2H, ArH), 4.17 (dd, J = 8.0 Hz, 2H) 4.03 (s, 1H, NH) ppm. $^{13}\text{C}\{^1\text{H}\}$ NMR (100 MHz, CDCl_3): δ 156.8 (ArC), 156.7 (ArC), 136.2 (ArC), 134.1 (ArC), 133.2 (ArC), 131.8 (ArC), 128.5 (ArC), 122.3 (ArC), 46.3 (CH₂) ppm. $^{31}\text{P}\{^1\text{H}\}$ NMR (161.9 MHz, CDCl_3): δ 57.6 ppm. ($\text{C}_{18}\text{H}_{17}\text{N}_2\text{PSe}$) (371.27), calcd C 58.23, H 4.62, N 7.55; found, C 57.93, H 4.45, N 7.38.

Preparation of $[\text{M}(\text{THF})_2(\text{Ph}_2\text{P}(\text{=E})\text{NCH}_2(\text{C}_5\text{H}_4\text{N}))]$ [M = Li, E = S (3a), Se (3b)]. Inside the glovebox, in a 10 mL sample vial, 1 equiv of 1-H or 2-H and 1 equiv of $[\text{LiN}(\text{SiMe}_3)_2]$ (23 mg, 0.134 mmol) were mixed together with 5 mL of THF and kept at room temperature. After 6 h, a small amount of THF (2 mL) and *n*-pentane (2 mL) were added onto it and kept at -35 °C. Colorless crystals of **3a** or **3b** were obtained.

3a; Yield: 75 mg (96%). ^1H NMR (400 MHz, C_6D_6): δ 8.12–8.03 (m, 5H, ArH), 7.02–7.01 (m, 6H, ArH), 6.87–6.86 (m, 1H, ArH), 6.49–6.48 (m, 2H, ArH), 4.54 (d, J = 8.0 Hz, 2H), 3.59 (m, THF), 1.41 (m, THF) ppm. $^{13}\text{C}\{^1\text{H}\}$ NMR (100 MHz, C_6D_6): δ 148.6 (Ar-C), 132.1 (Ar-C), 128.1 (Ar-C), 127.9 (Ar-C), 127.6 (Ar-C), 67.7 (THF), 46.3 (CH₂), 25.6 (THF) ppm. $^{31}\text{P}\{^1\text{H}\}$ NMR (161.9 MHz, C_6D_6): δ 69.5 ppm. ($\text{C}_{26}\text{H}_{32}\text{LiN}_2\text{O}_2\text{PS}$) (474.52), calcd C 65.81, H 6.80, N 5.90; found, C 65.43, H 6.54, N 5.62.

3b; Yield: 68 mg (91%). ^1H NMR (400 MHz, C_6D_6): δ 8.40–8.35 (m, 1H, ArH), 8.12–8.05 (m, 4H, ArH), 7.16–6.96 (m, 6H, ArH), 6.89–6.79 (m, 1H, ArH), 6.78–6.44 (m, 2H, ArH), 4.57 (d, J = 9.2

Hz, 2H) ppm. $^{13}\text{C}\{^1\text{H}\}$ NMR (100 MHz, C_6D_6): δ 148.6 (Ar-C), 132.1 (Ar-C), 131.3 (Ar-C), 131.9 (Ar-C), 127.9 (Ar-C), 121.9 (Ar-C), 121.8 (Ar-C) 67.7 (THF), 46.3 (CH₂), 25.6 (THF) ppm. $^{31}\text{P}\{^1\text{H}\}$ NMR (161.9 MHz, C_6D_6): δ 69.7 ppm. ($\text{C}_{26}\text{H}_{32}\text{LiN}_2\text{O}_2\text{PSe}$) (521.41), calcd C 59.89, H 6.19, N 5.37; found, C 59.61, H 5.92, N 5.01.

Preparation of $[\text{M}(\text{THF})_n(\text{Ph}_2\text{P}(\text{=E})\text{NCH}_2(\text{C}_5\text{H}_4\text{N}))_2]$ [M = Na, E = S(4a), Se (4b); M = K, E = Se (5b)]. Inside the glovebox, in a 20 mL sample vial, one equivalent of 1-H or 2-H and 1 equiv of $[\text{NaN}(\text{SiMe}_3)_2]$ (25 mg, 0.134 mmol) were mixed together with 5 mL of THF at room temperature. After 6 h, a small amount of THF (2 mL) and *n*-pentane (2 mL) was added onto it and kept at -35 °C. Colorless crystals of **4a** or **4b** were obtained.

4a; Yield: 75 mg (96%). ^1H NMR (400 MHz, C_6D_6): δ 8.30–8.26 (m, 2H, ArH), 8.10–8.06 (m, 8H, ArH), 7.03–7.02 (m, 12H, ArH), 6.87–6.84 (m, 2H, ArH), 6.52–6.48 (m, 4H, ArH), 4.32 (d, J = 8.0 Hz, 4H), 3.49 (br, THF), 1.30 (br, THF) ppm. $^{13}\text{C}\{^1\text{H}\}$ NMR (100 MHz, C_6D_6): δ 148.6 (Ar-C), 132.1 (Ar-C), 128.1 (Ar-C), 127.9 (Ar-C), 127.6 (Ar-C), 67.7 (THF), 46.3 (CH₂), 25.6 (THF) ppm. $^{31}\text{P}\{^1\text{H}\}$ NMR (161.9 MHz, C_6D_6): δ 68.5 ppm. ($\text{C}_{44}\text{H}_{48}\text{N}_4\text{Na}_2\text{O}_2\text{P}_2\text{S}_2$) (836.9), calcd C 63.14, H 5.78, N 6.69; found, C 62.83, H 5.54, N 6.45.

4b; Yield: 116 mg (93%). ^1H NMR (400 MHz, C_6D_6): δ 8.08–8.05 (m, 2H, ArH), 8.04–8.02 (m, 8H, ArH), 6.95–6.92 (m, 12H, ArH), 6.90–6.84 (m, 2H, ArH), 6.52–6.48 (m, 4H, ArH), 4.18 (d, J = 9.2 Hz, 4H) ppm. $^{13}\text{C}\{^1\text{H}\}$ NMR (100 MHz, C_6D_6): δ 131.8 (ArC), 130.8 (ArC), 128.4 (ArC), 127.9 (ArC), 127.6 (ArC), 127.1 (ArC), 67.7 (THF), 25.6 (THF) ppm. $^{31}\text{P}\{^1\text{H}\}$ NMR (161.9 MHz, C_6D_6): δ 70.4 ppm. ($\text{C}_{44}\text{H}_{48}\text{N}_4\text{Na}_2\text{O}_2\text{P}_2\text{Se}_2$) (930.70), calcd C 56.78, H 5.20, N 6.02; found, C 56.36, H 4.96, N 5.81.

Complex **5b** was prepared in an analogous method described for complexes **4a** and **4b** by using 1 equiv (50 mg, 0.134 mmol) of 2-H and 1 equiv of $[\text{KN}(\text{SiMe}_3)_2]$ (27 mg, 0.134 mmol).

5b; Yield: 135 mg (90%). ^1H NMR (400 MHz, C_6D_6): δ 8.24–8.13 (m, 5H, ArH), 7.02–6.98 (m, 6H, ArH), 6.90–6.86 (m, 1H, ArH), 6.56–6.50 (m, 2H, ArH), 4.26 (d, J = 9.2 Hz, 4H) ppm. $^{13}\text{C}\{^1\text{H}\}$ NMR (100 MHz, C_6D_6): δ 131.8 (ArC), 130.8 (ArC), 128.4 (P attached o-ArC), 127.9 (P attached p-ArC), 127.6 (ArC), 127.1 (ArC), 67.7 (THF), 25.6 (THF) ppm. $^{31}\text{P}\{^1\text{H}\}$ NMR (161.9 MHz, C_6D_6): δ 70.7 ppm. ($\text{C}_{52}\text{H}_{64}\text{K}_2\text{N}_4\text{O}_4\text{P}_2\text{Se}_2$) (1107.13), calcd C 56.41, H 5.83, N 5.06; found, C 56.12, H 5.49, N 4.73.

Preparation of $[\kappa^2\text{-(Ph}_2\text{P}(\text{=Se})\text{NCH}_2(\text{C}_5\text{H}_4\text{N}))\text{Mg}(\text{THF})]$ (6b). Inside the glovebox, in a 25 mL predried Schlenk flask, compound **2H** (50 mg, 0.134 mmol) was mixed with 27 mg of $[\text{KN}(\text{SiMe}_3)_2]$ and 19 mg of MgI_2 (0.0672 mmol) in 10 mL THF solvent at ambient temperature and the reaction mixture was stirred for 8 h. The white precipitate of KI was filtered off, and the filtrate was evaporated under reduced pressure. The resulting white residue was further purified by washing with pentane and was recrystallized from THF-pentane (1:2 ratio) mixture at -35 °C.

Yield: 95 mg (92%). ^1H NMR (400 MHz, C_6D_6): δ 8.39 (m, 2H), 8.32–8.29 (m, 7H, ArH), 7.32 (s, 2H, ArH), 7.32–7.08 (m, 14H, ArH), 6.57–6.50 (m, 4H, ArH), 4.44 (d, J = 9 Hz, 4H) ppm. $^{13}\text{C}\{^1\text{H}\}$

NMR (100 MHz, C_6D_6): δ 148.6 (Ar–C), 132.1 (Ar–C), 131.3 (Ar–C), 131.9 (Ar–C), 127.9 (Ar–C), 121.9 (Ar–C), 121.8 (Ar–C), 46.5 (CH_2) ppm. $^{31}P\{^1H\}$ NMR (161.9 MHz, C_6D_6): δ 70.6 ppm. ($C_{40}H_{40}MgN_4OP_2Se_2$) (836.94), calcd C 57.40, H 4.82, N 6.69; found, C 57.17, H 4.52, N 6.46.

Preparation of $[\kappa^3\text{-}(\text{Ph}_2\text{P}(\text{=Se})\text{NCH}_2(\text{C}_5\text{H}_4\text{N}))_2\text{M}(\text{THF})_2]$ [M = Ca (7b), Sr (8b), Ba(9b)]. Inside the glovebox, in a 25 mL predried Schlenk flask, compound 2H was mixed with $[\text{KN}(\text{SiMe}_3)_2]$ and alkaline earth metal diiodide (2:2:1 ratio) in 10 mL of THF at ambient temperature, and the reaction mixture was stirring for 8 h. The white precipitate of KI was filtered off, and the filtrate was evaporated under reduced pressure. The resulting white compound was further purified by washing with pentane and was recrystallized from the THF–pentane (1:2 ratio) mixture at -35°C .

M = Ca (7b): Yield: (94%). ^1H NMR (400 MHz, C_6D_6): δ 8.18–8.12 (m, 10H, ArH), 7.01–6.99 (m, 12H, ArH), 6.90–6.88 (m, 2H, ArH), 6.55–6.49 (m, 4H, ArH), 4.26 (d, $J = 8.4$ Hz, 4H), 3.60–3.54 (m, THF), 1.42–1.39 (m, THF) ppm. $^{13}C\{^1H\}$ NMR (100 MHz, C_6D_6): δ 148.7 (ArC), 136.1 (ArC), 132.2 (ArC), 132.1 (Ar–C), 131.5 (Ar–C) 127.9 (ArC), 122.7 (ArC), 121.9 (ArC), 67.8 (THF), 46.4 (CH_2), 25.7 (THF) ppm. $^{31}P\{^1H\}$ NMR (161.9 MHz, C_6D_6): δ 71.0 ppm. ($C_{44}H_{48}CaN_4O_2P_2Se_2$) (924.8), calcd C 57.14, H 5.23, N 6.06; found, C 56.79, H 5.11, N 5.81.

M = Sr (8b): Yield: (91%). ^1H NMR (400 MHz, C_6D_6): δ 8.24–8.18 (d, $J = 4.6$ Hz, 2H), 8.16–8.12 (m, 8H, ArH), 7.01–6.98 (m, 12H, ArH), 6.91–6.83 (m, 2H, ArH), 6.58–6.56 (m, 4H, ArH), 4.26 (d, $J = 9$ Hz, 4H), 3.60–3.54 (m, THF), 1.42–1.39 (m, THF) ppm. $^{13}C\{^1H\}$ NMR (100 MHz, C_6D_6): δ 148.6 (Ar–C), 132.1 (Ar–C), 131.3 (Ar–C), 131.9 (Ar–C), 127.9 (Ar–C), 121.9 (Ar–C), 121.8 (Ar–C) 67.7 (THF), 46.3 (CH_2), 25.6 (THF) ppm. $^{31}P\{^1H\}$ NMR (161.9 MHz, C_6D_6): δ 70.9 ppm. ($C_{44}H_{48}SrN_4O_2P_2Se_2$) (972.3), calcd C 54.35, H 4.98, N 5.76; found, C 53.91, H 4.76, N 5.49.

M = Ba (9b): Yield: (94%). ^1H NMR (400 MHz, C_6D_6): δ 8.08 (d, $J = 4.6$ Hz, 2H), 8.07–8.03 (m, 8H, ArH), 6.90–6.88 (m, 12H, ArH), 6.89–6.78 (m, 2H, ArH), 6.46–6.44 (m, 4H, ArH), 4.16 (d, $J = 8.4$ Hz, 4H), 3.60–3.54 (m, THF), 1.42–1.39 (m, THF) ppm. $^{13}C\{^1H\}$ NMR (100 MHz, C_6D_6): δ 148.6 (ArC), 135.9 (ArC), 132.1 (ArC), 132.0 (Ar–C), 131.3 (Ar–C) 127.9 (P attached p-ArC), 121.9 (ArC), 121.8 (ArC), 67.7 (THF), 46.3 (CH_2), 25.6 (THF) ppm. $^{31}P\{^1H\}$ NMR (161.9 MHz, C_6D_6): δ 70.9 ppm. ($C_{44}H_{48}BaN_4O_2P_2Se_2$) (1022.07). calcd C 51.71, H 4.73, N 5.48; found, C 51.41, H 4.35, N 5.33

■ ASSOCIATED CONTENT

Supporting Information

The Supporting Information is available free of charge on the ACS Publications website at DOI: 10.1021/acs.inorgchem.7b02847.

^1H NMR, $^{13}C\{^1H\}$, and $^{31}P\{^1H\}$ NMR spectra of all the complexes and full details of the single crystal X-ray diffraction analyses of the reported complexes 1-H, 2-H, 3a, 3b, 4a, 4b, 5b, 6b, 7b, 8b and 9b; all the details of ROP of *rac* LA, *e*-CL, and copolymerization of *rac* LA and *e*-CL (PDF)

Accession Codes

CCDC 1582994–1583002 contain the supplementary crystallographic data for this paper. These data can be obtained free of charge via www.ccdc.cam.ac.uk/data_request/cif, or by emailing data_request@ccdc.cam.ac.uk, or by contacting The Cambridge Crystallographic Data Centre, 12 Union Road, Cambridge CB2 1EZ, UK; fax: +44 1223 336033.

■ AUTHOR INFORMATION

Corresponding Author

*E-mail: tpanda@iith.ac.in.

ORCID

Hari Pada Nayek: 0000-0003-4247-547X

Tarun K. Panda: 0000-0003-0975-0118

Author Contributions

All the authors contributed equally.

Notes

The authors declare no competing financial interest.

■ ACKNOWLEDGMENTS

This work was supported by the Science and Engineering Research Board (SERB), Department of Science and Technology (DST), India, under project no. (EMR/2016/005150). A. H. and J. B. thank CSIR and UGC India respectively for their Ph.D. fellowships. We thank Prof. Kazushi Mashima and Dr. Hayato Tsurugi, Osaka University, Japan, for their generous support.

■ REFERENCES

- (1) Madhavan, N. K.; Nair, N. R.; John, R. P. An overview of the recent developments in polylactide (PLA) research. *Bioresour. Technol.* **2010**, *101*, 8493–8501.
- (2) Inkinen, S.; Hakkarainen, M.; Albertsson, A. C.; Sodergard, A. From Lactic Acid to Poly(lactic acid) (PLA): Characterization and Analysis of PLA and Its Precursors. *Biomacromolecules* **2011**, *12*, 523–532.
- (3) Hutchinson, M. H.; Dorgan, J. R.; Knauss, D. M.; Hait, S. B. Optical Properties of Poly(lactides). *J. Polym. Environ.* **2006**, *14*, 119–124.
- (4) Ikada, Y.; Tsuji, H. Biodegradable polyesters for medical and ecological applications. *Macromol. Rapid Commun.* **2000**, *21*, 117–132.
- (5) Vink, E. T. H.; Rábago, K. R.; Glassner, D. A.; Springs, B.; O'Connor, R. P.; Kolstad, J.; Gruber, P. R. The Sustainability of NatureWorks Poly(lactide) Polymers and Ingeo Poly(lactide) Fibers: an Update of the Future. *Macromol. Biosci.* **2004**, *4*, 551–564.
- (6) Blanco, I. End-life prediction of commercial PLA used for food packaging through short term TGA experiments: Real chance or low reliability. *Chin. J. Polym. Sci.* **2014**, *32*, 681–689.
- (7) Morschbacker, A. Bio-Ethanol Based Ethylene. *Polym. Rev.* **2009**, *49*, 79–84.
- (8) O'Keefe, B. J.; Hillmyer, M. A.; Tolman, W. B. Polymerization of lactide and related cyclic esters by discrete metal complexes. *J. Chem. Soc., Dalton Trans.* **2001**, 2215–2224.
- (9) Dechy-Cabaret, O.; Martin-Vaca, B. M.; Bourissou, D. Controlled Ring-Opening Polymerization of Lactide and Glycolide. *Chem. Rev.* **2004**, *104*, 6147–6176.
- (10) Ajellal, N.; Carpentier, J.; Guillaume, C.; Guillaume, S. M.; Helou, M.; Poirier, V.; Sarazin, Y.; Trifonov, A. Metal-catalyzed immortal ring-opening polymerization of lactones, lactides and cyclic carbonates. *Dalton Trans.* **2010**, 39, 8363–8376.
- (11) Thomas, C. M.; Lutz, J. F. Precision Synthesis of Biodegradable Polymers. *Angew. Chem., Int. Ed.* **2011**, *50*, 9244–9246.
- (12) Castillo, J. A.; Borchmann, D. E.; Cheng, A. Y.; Wang, Y.; Hu, C.; García, A. J.; Weck, M. Well-Defined Poly(lactic acid)s Containing Poly(ethylene glycol) Side Chains. *Macromolecules* **2012**, *45*, 62–69.
- (13) Makiguchi, K.; Ogasawara, Y.; Kikuchi, S.; Satoh, T.; Kakuchi, T. Diphenyl Phosphate as an Efficient Acidic Organocatalyst for Controlled/Living Ring-Opening Polymerization of Trimethylene Carbonates Leading to Block, End-Functionalized, and Macrocyclic Polycarbonates. *Macromolecules* **2013**, *46*, 1772–1782.
- (14) Todd, R.; Rubio, G.; Hall, D. J.; Tempelaar, S.; Dove, A. P. Benzyl bispidine as an efficient replacement for (–)-sparteine in ring opening polymerization. *Chem. Sci.* **2013**, *4*, 1092–1097.
- (15) Nimitsirawat, N.; Gibson, V. C.; Marshall, E. L.; Elsegood, M. R. Bidentate salicylaldiminato tin(II) complexes and their use as lactide polymerisation initiators. *Dalton Trans.* **2009**, 3710–3715.

- (16) Nimitsiriwat, N.; Gibson, V. C.; Marshall, E. L.; Elsegood, M. R. The Reversible Amination of Tin(II)-Ligated Imines: Latent Initiators for the Polymerization of rac-Lactide. *Inorg. Chem.* **2008**, *47*, 5417–5424.
- (17) Pilone, A.; Press, K.; Goldberg, I.; Kol, M.; Mazzeo, M.; Lamberti, M. Gradient Isotactic Multiblock Poly lactides from Aluminum Complexes of Chiral Salalen Ligands. *J. Am. Chem. Soc.* **2014**, *136*, 2940–2943.
- (18) Pang, X.; Duan, R.; Li, X.; Chen, X. Bimetallic salen–aluminum complexes: synthesis, characterization and their reactivity with rac-lactide and ϵ -caprolactone. *Polym. Chem.* **2014**, *5*, 3894–3900.
- (19) Meduri, A.; Fuoco, T.; Lamberti, M.; Pellicchia, C.; Pappalardo, D. Versatile Copolymerization of Glycolide and rac-Lactide by Dimethyl(salicylaldiminato)aluminum Compounds. *Macromolecules* **2014**, *47*, 534–543.
- (20) Honrado, M.; Otero, A.; Fernández-Baeza, J.; Sánchez-Barba, L. F.; Garcés, A.; Lara-Sánchez, A.; Rodríguez, A. M. Stereoselective ROP of rac-Lactide Mediated by Enantiopure NNO-Scorpionate Zinc Initiators. *Organometallics* **2014**, *33*, 1859–1866.
- (21) Wang, H.; Ma, H. Highly diastereoselective synthesis of chiral aminophenolate zinc complexes and isoselective polymerization of rac-lactide. *Chem. Commun.* **2013**, *49*, 8686–8688.
- (22) Yi, W.; Ma, H. Magnesium complexes containing biphenyl-based tridentate imino-phenolate ligands for ring-opening polymerization of rac-lactide and α -methyltrimethylene carbonate. *Dalton Trans.* **2014**, *43*, 5200–5210.
- (23) Garcés, A.; Sánchez-Barba, L. F.; Fernández-Baeza, J.; Otero, A.; Honrado, M.; Lara-Sánchez, A.; Rodríguez, A. M. Heteroscorpionate Magnesium Alkyls Bearing Unprecedented Apical σ -C(sp³)–Mg Bonds: Heteroselective Ring-Opening Polymerization of rac-Lactide. *Inorg. Chem.* **2013**, *52*, 12691–12701.
- (24) Gorczynski, J. L.; Chen, J.; Fraser, C. L. Iron Tris-(dibenzoylmethane)-Centered Poly lactide Stars: Multiple Roles for the Metal Complex in Lactide Ring-Opening Polymerization. *J. Am. Chem. Soc.* **2005**, *127*, 14956–14957.
- (25) Giese, S. O.; Egevardt, C.; Rüdiger, A. L.; Sá, E. L.; Silva, T. A.; Zawadzki, S. F.; Soares, J. F.; Nunes, G. G. Catalytic Activity of a Titanium(IV)/Iron(II) Heterometallic Alkoxide in the Ring-Opening Polymerization of ϵ -Caprolactone and rac-Lactide. *J. Braz. Chem. Soc.* **2015**, *26*, 2258–2268.
- (26) Gao, B.; Li, X.; Duan, R.; Pang, X. Titanium complexes with octahedral geometry chelated by salen ligands adopting β -cis configuration for the ring-opening polymerisation of lactide. *New J. Chem.* **2015**, *39*, 2404–2408.
- (27) Tsai, C.; Du, H.; Chang, J.; Huang, B.; Ko, B.; Lin, C. Ring-opening polymerization of cyclic esters initiated by zirconium, titanium and yttrium complexes. *RSC Adv.* **2014**, *4*, 14527–14537.
- (28) Douglas, A. F.; Patrick, B. O.; Mehrkhodavandi, P. A highly active chiral indium catalyst for living lactide polymerization. *Angew. Chem.* **2008**, *120*, 2322–2325.
- (29) Platel, R. H.; White, A. J. P.; Williams, C. K. Bis(phosphinic)-diamido Yttrium Amide, Alkoxide, and Aryloxide Complexes: An Evaluation of Lactide Ring-Opening Polymerization Initiator Efficiency. *Inorg. Chem.* **2011**, *50*, 7718–7728.
- (30) Liu, B.; Roisnel, T.; Maron, L.; Carpentier, J.; Sarazin, Y. Discrete Divalent Rare-Earth Cationic ROP Catalysts: Ligand-Dependent Redox Behavior and Discrepancies with Alkaline-Earth Analogues in a Ligand-Assisted Activated Monomer Mechanism. *Chem. - Eur. J.* **2013**, *19*, 3986–3994.
- (31) Guillaume, S. M.; Maron, L.; Roesky, P. W. Catalytic Behavior of Rare-Earth Borohydride Complexes in Polymerization of Polar Monomers. *Handbook on the Physics and Chemistry of Rare Earths* **2014**, *44*, 1–86.
- (32) Kadota, J.; Pavlović, D.; Hirano, H.; Okada, A.; Agari, Y.; Bibal, B.; Defieux, A.; Peruch, F. Controlled bulk polymerization of L-lactide and lactones by dual activation with organo-catalytic systems. *RSC Adv.* **2014**, *4*, 14725–14732.
- (33) Ma, H.; Spaniol, T. P.; Okuda, J. Highly Heteroselective Ring-Opening Polymerization of rac-Lactide Initiated by Bis(phenolato)-scandium Complexes. *Angew. Chem., Int. Ed.* **2006**, *45*, 7818–7821.
- (34) Walsh, P. J.; Lurain, A. E.; Balsells, J. Use of Achiral and Meso Ligands To Convey Asymmetry in Enantioselective Catalysis. *Chem. Rev.* **2003**, *103*, 3297–3344.
- (35) Jhurry, D.; Luximon, A. B.; Spassky, N. *Macromol. Symp.* **2001**, *175*, 67–80.
- (36) Majerska, K.; Duda, A. Stereocontrolled Polymerization of Racemic Lactide with Chiral Initiator: Combining Stereoselection and Chiral Ligand-Exchange Mechanism. *J. Am. Chem. Soc.* **2004**, *126*, 1026–1027.
- (37) Du, H.; Velders, A. H.; Dijkstra, P. J.; Sun, J.; Zhong, Z.; Chen, X.; Feijen, J. Chiral Salan Aluminium Ethyl Complexes and Their Application in Lactide Polymerization. *Chem. - Eur. J.* **2009**, *15*, 9836–9845.
- (38) Bouyahyi, M.; Grunova, E.; Marquet, N.; Kirillov, E.; Thomas, C. M.; Roisnel, T.; Carpentier, J. Aluminum Complexes of Fluorinated Dialkoxy-Diimino Salen-like Ligands: Syntheses, Structures, and Use in Ring-Opening Polymerization of Cyclic Esters. *Organometallics* **2008**, *27*, 5815–5825.
- (39) Bouyahyi, M.; Roisnel, T.; Carpentier, J. Aluminum Complexes of Bidentate Fluorinated Alkoxy-Imino Ligands: Syntheses, Structures, and Use in Ring-Opening Polymerization of Cyclic Esters. *Organometallics* **2012**, *31*, 1458–1466.
- (40) Bakewell, C.; Platel, R. H.; Cary, S. K.; Hubbard, S. M.; Roaf, J. M.; Levine, A. C.; White, A. J.; Long, N. J.; Haaf, M.; Williams, C. K. Bis(8-quinolinolato)aluminum ethyl complexes: Iso-Selective Initiators for rac-Lactide Polymerization. *Organometallics* **2012**, *31*, 4729–4736.
- (41) Chen, H.; Dutta, S.; Huang, P.; Lin, C. Preparation and Characterization of Aluminum Alkoxides Coordinated on salen-Type Ligands: Highly Stereoselective Ring-Opening Polymerization of rac-Lactide. *Organometallics* **2012**, *31*, 2016–2025.
- (42) Bakewell, C.; White, A. J.; Long, N. J.; Williams, C. K. 8-Quinolinolato Gallium Complexes: Iso-selective Initiators for rac-Lactide Polymerization. *Inorg. Chem.* **2013**, *52*, 12561–12567.
- (43) Normand, M.; Dorcet, V.; Kirillov, E.; Carpentier, J. {Phenoxy-imine}aluminum versus -indium Complexes for the Immortal ROP of Lactide: Different Stereocontrol, Different Mechanisms. *Organometallics* **2013**, *32*, 1694–1709.
- (44) Hild, F.; Neehaul, N.; Bier, F.; Wirsum, M.; Gourlaouen, C.; Dagonne, S. Synthesis and Structural Characterization of Various N₂O₂-Chelated Aluminum and Gallium Complexes for the Efficient ROP of Cyclic Esters and Carbonates: How Do Aluminum and Gallium Derivatives Compare? *Organometallics* **2013**, *32*, 587–598.
- (45) Nomura, N.; Ishii, R.; Akakura, M.; Aoi, K. Stereoselective Ring-Opening Polymerization of Racemic Lactide Using Aluminum-Achiral Ligand Complexes: Exploration of a Chain-End Control Mechanism. *J. Am. Chem. Soc.* **2002**, *124*, 5938–5939.
- (46) Nomura, N.; Ishii, R.; Yamamoto, Y.; Kondo, T. Stereoselective Ring-Opening Polymerization of a Racemic Lactide by Using Achiral Salen- and Homosalen-Aluminum Complexes. *Chem. - Eur. J.* **2007**, *13*, 4433–4451.
- (47) Nomura, N.; Akita, A.; Ishii, R.; Mizuno, M. Random Copolymerization of ϵ -Caprolactone with Lactide Using a Homosalen-Al Complex. *J. Am. Chem. Soc.* **2010**, *132*, 1750–1751.
- (48) Gao, B.; Duan, R.; Pang, X.; Li, X.; Qu, Z.; Tang, Z.; Zhuang, X.; Chen, X. Stereoselective Ring-Opening Polymerization of rac-Lactides Catalyzed by Aluminum Hemi-Salen Complexes. *Organometallics* **2013**, *32*, 5435–5444.
- (49) Cross, E. D.; Allan, L. E.; Decken, A.; Shaver, M. P. Aluminum salen and salan complexes in the ring-opening polymerization of cyclic esters: Controlled immortal and copolymerization of rac- β -butyrolactone and rac-lactide. *J. Polym. Sci., Part A: Polym. Chem.* **2013**, *51*, 1137–1146.
- (50) Aluthge, D. C.; Patrick, B. O.; Mehrkhodavandi, P. A highly active and site selective indium catalyst for lactide polymerization. *Chem. Commun.* **2013**, *49*, 4295–4297.

- (51) Hancock, S. L.; Mahon, M. F.; Jones, M. D. Salen complexes based on 1,4-diaminocyclohexane and their exploitation for the polymerisation of rac-lactide. *New J. Chem.* **2013**, *37*, 1996–2001.
- (52) Shen, Y.; Zhu, K. J.; Shen, Z.; Yao, K. M. Synthesis and characterization of highly random copolymer of ϵ -caprolactone and D,L-lactide using rare earth catalyst. *J. Polym. Sci., Part A: Polym. Chem.* **1996**, *34*, 1799–1805.
- (53) Van Butsele, K. V.; Jérôme, R.; Jérôme, C. Functional amphiphilic and biodegradable copolymers for intravenous vectorization. *Polymer* **2007**, *48*, 7431–7443.
- (54) Lahcini, M.; Castro, P. M.; Kalmi, M.; Leskela, M.; Repo, T. The Use of Tetra(phenylethynyl)titanium as an Initiator for the Ring-Opening Polymerization of Lactide. *Organometallics* **2004**, *23*, 4547–4549.
- (55) Wang, J.; Dong, C. Synthesis, Sequential Crystallization and Morphological Evolution of Well-Defined Star-Shaped Poly(ϵ -caprolactone)-*b*-poly(L-lactide) Block Copolymer. *Macromol. Chem. Phys.* **2006**, *207*, 554–562.
- (56) Vanhoorne, P.; Dubois, P.; Jerome, R.; Teyssie, P. Macromolecular engineering of polylactones and polylactides. 7. Structural analysis of copolyesters of ϵ -caprolactone and L- or D,L-lactide initiated by triisopropoxyaluminum. *Macromolecules* **1992**, *25*, 37–44.
- (57) Bero, M.; Kasperczyk, J. Coordination polymerization of lactides, Influence of lactide structure on the transesterification processes in the copolymerization with ϵ -caprolactone. *Macromol. Chem. Phys.* **1996**, *197*, 3251–3258.
- (58) Huang, M.; Li, S.; Coudane, J.; Vert, M. Synthesis and Characterization of Block Copolymers of ϵ -Caprolactone and DL-Lactide Initiated by Ethylene Glycol or Poly(ethylene glycol). *Macromol. Chem. Phys.* **2003**, *204*, 1994.
- (59) Chmura, A. J.; Davidson, M. G.; Jones, M. D.; Lunn, M. D.; Mahon, M. F.; Johnson, A. F.; Khunkamchoo, P.; Roberts, S. L.; Wong, S. S. F. Group 4 Complexes with Aminebisphenolate Ligands and Their Application for the Ring Opening Polymerization of Cyclic Esters. *Macromolecules* **2006**, *39*, 7250–7257.
- (60) Dakshinamoorthy, D.; Peruch, F. Block and random copolymerization of ϵ -caprolactone, L-, and rac-lactide using titanium complex derived from aminodiol ligand. *J. Polym. Sci., Part A: Polym. Chem.* **2012**, *50*, 2161.
- (61) Grijpma, D. W.; Pennings, A. J. Polymerization temperature effects on the properties of l-lactide and ϵ -caprolactone copolymers. *Polym. Bull.* **1991**, *25*, 335–341.
- (62) Stanlake, L. J. E.; Beard, J. D.; Schafer, L. L. Rare-Earth Amidate Complexes. Easily Accessed Initiators For ϵ -Caprolactone Ring-Opening Polymerization. *Inorg. Chem.* **2008**, *47*, 8062–8068.
- (63) Webster, R. L.; Noroozi, N.; Hatzikiriakos, S. G.; Thomson, J. A.; Schafer, L. L. Titanium pyridonates and amidates: novel catalysts for the synthesis of random copolymers. *Chem. Commun.* **2013**, *49*, 57–59.
- (64) Della Monica, F.; Luciano, E.; Roviello, G.; Grassi, A.; Milione, S.; Capacchione, C. Group 4 Metal Complexes Bearing Thioetherphenolate Ligands. Coordination Chemistry and Ring-Opening Polymerization Catalysis. *Macromolecules* **2014**, *47*, 2830–2841.
- (65) García-Valle, F. M.; Estivill, R.; Gallegos, C.; Cuenca, T.; Mosquera, M. E. G.; Taberner, V.; Cano, J. Metal and Ligand-Substituent Effects in the Immortal Polymerization of rac-Lactide with Li, Na, and K Phenoxo-imine Complexes. *Organometallics* **2015**, *34*, 477–487.
- (66) Huang, Y.; Wang, W.; Lin, C.-C.; Blake, M. P.; Clark, L. A.; Schwarz, D.; Mountford, P. Potassium, zinc, and magnesium complexes of a bulky OOO-tridentate bis(phenolate) ligand: synthesis, structures, and studies of cyclic ester polymerization. *Dalton Trans.* **2013**, *42*, 9313–9324.
- (67) Roşca, S. C.; Roşca, D.-A.; Dorcet, V.; Kozak, C. M.; Kerton, F. M.; Carpentier, J.-F.; Sarazin, Y. Alkali aminoether-phenolate complexes: synthesis, structural characterization and evidence for an activated monomer ROP mechanism. *Dalton Trans.* **2013**, *42*, 9361–9375.
- (68) Zhang, J.; Jian, C.; Gao, Y.; Wang, L.; Tang, N.; Wu, J. Synthesis and Characterization of Multi-Alkali-Metal Tetraphenolates and Application in Ring-Opening Polymerization of Lactide. *Inorg. Chem.* **2012**, *51*, 13380–13389.
- (69) Chen, H.-Y.; Zhang, J. B.; Lin, C.-C.; Reibenspies, J. H.; Miller, S. A. Efficient and controlled polymerization of lactide under mild conditions with a sodium-based catalyst. *Green Chem.* **2007**, *9*, 1038–1040.
- (70) Bhattacharjee, J.; Harinath, A.; Nayek, H. P.; Sarkar, A.; Panda, T. K. Highly Active and Iso-selective Catalysts for ROP of Cyclic Esters Using Group 2 Metal Initiators. *Chem. - Eur. J.* **2017**, *23*, 9319–9331.
- (71) Milton, H. L.; Wheatley, M. V.; Slawin, A. M. Z.; Woollins, J. D. Synthesis and coordination of 2-diphenylphosphinocolinamide. *Polyhedron* **2004**, *23*, 3211–3220.
- (72) Kottalanka, R. K.; Adimulam, H.; Bhattacharjee, J.; Babu, H. V.; Panda, T. K. Bis(phosphinoselenoic amides) as Versatile Chelating Ligands for Alkaline Earth Metal (Mg, Ca, Sr and Ba) Complexes: Syntheses, Structure and ϵ -Caprolactone Polymerisation. *Dalton Trans.* **2014**, *43*, 8757–8766.
- (73) Kottalanka, R. K.; Naktode, K.; Anga, S.; Nayek, H. P.; Panda, T. K. Heavier Alkaline Earth metal Complexes with Phosphinoselenoic amides: Evidence of Direct M-Se Contact (M = Ca, Sr and Ba). *Dalton Trans.* **2013**, *42*, 4947–4956.
- (74) Panda, T. K.; Gamer, M. T.; Roesky, P. W. Syntheses and structures of calcium and ytterbium Bis(diphosphanyl-amido) complex. *Inorg. Chim. Acta* **2006**, *359*, 4765–4768.
- (75) Gindelberger, D. E.; Arnold, J. Preparation and Properties of Magnesium, Calcium, Strontium, and Barium Selenolates and Tellurolates. *Inorg. Chem.* **1994**, *33*, 6293–6299.
- (76) Kling, C.; Ott, H.; Schwab, G.; Stalke, D. Heteroaromatic Substituted Phosphoranes with Enhanced Hemilabile Character. *Organometallics* **2008**, *27*, 5038–5042.
- (77) Ruhlandt-Senge, K.; Englich, U. Barium Thiulates and Selenolates: Syntheses and Structural Principles. *Chem. - Eur. J.* **2000**, *6*, 4063–4070.
- (78) Bhattacharjee, J.; Das, S.; Reddy, Th. D. N.; Mallik, B. S.; Panda, T. K.; Nayek, H. P. Alkali Metal and Alkaline Earth Metal Complexes of Bis(diphenylphosphino-borane)amido Ligand – Synthesis, Structures and Catalysis for Ring-Opening Polymerization of ϵ -Caprolactone. *Z. Anorg. Allg. Chem.* **2016**, *642*, 118–127.
- (79) Kottalanka, R. K.; Harinath, A.; Rej, S.; Panda, T. K. Group 1 and Group 2 Metal Complexes Supported by Bidentate Bulky Iminopyrrolyl Ligand: Synthesis, Structural Diversity, and ϵ -Caprolactone Polymerization Study. *Dalton Trans.* **2015**, *44*, 19865–19879.
- (80) Kottalanka, R. K.; Harinath, A.; Panda, T. K. Chiral Alkaline-Earth Metal Complexes Having M-Se Direct Bond (M = Mg, Ca, Sr, Ba): Syntheses, Structures and ϵ -Caprolactone Polymerisation. *RSC Adv.* **2015**, *5*, 37755–37767.
- (81) Hanusa, T. P. Non-cyclopentadienyl organometallic compounds of calcium, strontium and barium. *Coord. Chem. Rev.* **2000**, *210*, 329–367.
- (82) Westerhausen, M. Synthesis and Spectroscopic Properties of Bis(trimethylsilyl)amides of the Alkaline-Earth Metals Magnesium, Calcium, Strontium, and Barium. *Inorg. Chem.* **1991**, *30*, 96–101.
- (83) Harder, S.; Lutz, M. The Phosphonium Dibenzylidene Anion as a Ligand in Organobarium Chemistry. *Organometallics* **1997**, *16*, 225–230.
- (84) Crimmin, M. R.; Barrett, A. G.; Hill, M. S.; MacDougall, D. J.; Mahon, M. F.; Procopiou, P. A. Bis(trimethylsilyl)methyl Derivatives of Calcium, Strontium and Barium: Potentially Useful Dialkyls of the Heavy Alkaline Earth Elements. *Chem. - Eur. J.* **2008**, *14*, 11292–11295.
- (85) Addison, A. W.; Rao, T. N.; Reedijk, J.; van Rijn, J. V.; Verschoor, G. C. Synthesis, structure, and spectroscopic properties of copper(II) compounds containing nitrogen-sulphur donor ligands; the crystal and molecular structure of aqua[1,7-bis(N-methylbenzimidazol-2'-yl)-2,6-dithiaheptane]copper(II) perchlorate. *J. Chem. Soc., Dalton Trans.* **1984**, 1349–1356.

(86) Sarazin, Y.; Carpentier, J. F. Discrete Cationic Complexes for Ring-Opening Polymerization Catalysis of Cyclic Esters and Epoxides. *Chem. Rev.* **2015**, *115*, 3564–3614.

(87) Otera, J. Transesterification. *Chem. Rev.* **1993**, *93*, 1449–1470.

(88) Ouchi, M.; Terashima, T.; Sawamoto, M. Transition Metal-Catalyzed Living Radical Polymerization: Toward Perfection in Catalysis and Precision Polymer Synthesis. *Chem. Rev.* **2009**, *109*, 4963–5050.

(89) Makiguchi, K.; Yamanaka, T.; Kakuchi, T.; Terada, M.; Satoh, T. Binaphthol-derived phosphoric acids as efficient chiral organocatalysts for the enantiomer-selective polymerization of rac-lactide. *Chem. Commun.* **2014**, *50*, 2883–2885.

(90) Radano, C. P.; Baker, G. L.; Smith, M. R. Stereoselective Polymerization of a Racemic Monomer with a Racemic Catalyst: Direct Preparation of the Polylactic Acid Stereo complex from Racemic Lactide. *J. Am. Chem. Soc.* **2000**, *122*, 1552–1553.

(91) Bakewell, C.; White, A. J.; Long, N. J.; Williams, C. K. Metal-Size Influence in Iso-Selective Lactide Polymerization. *Angew. Chem., Int. Ed.* **2014**, *53*, 9226–9230.

(92) El-Zoghbi, I.; Whitehorne, T. J. J.; Schaper, F. Exceptionally high lactide polymerization activity of zirconium complexes with bridged diketiminate ligands. *Dalton Trans.* **2013**, *42*, 9376–9387.

(93) Whitelaw, E. L.; Davidson, M. G.; Jones, M. D. Group 4 salalen complexes for the production and degradation of polylactide. *Chem. Commun.* **2011**, *47*, 10004–10006.

(94) Romain, C.; Heinrich, B.; Laponnaz, S. B.; Dagorne, S. A robust zirconium N-heterocyclic carbene complex for the living and highly stereoselective ring-opening polymerization of rac-lactide. *Chem. Commun.* **2012**, *48*, 2213–2215.

(95) Schwarz, A. D.; Thompson, A. L.; Mountford, P. Sulfonamide-Supported Group 4 Catalysts for the Ring-Opening Polymerization of ϵ -Caprolactone and rac-Lactide. *Inorg. Chem.* **2009**, *48*, 10442–10454.

(96) Darensbourg, D. J.; Choi, W.; Karroonnirun, O.; Bhuvanesh, N. Ring-Opening Polymerization of Cyclic Monomers by Complexes Derived from Biocompatible Metals. Production of Poly(lactide), Poly(trimethylene carbonate), and Their Copolymers. *Macromolecules* **2008**, *41*, 3493–3502.

(97) Yu, I.; Acosta-Ramírez, I.; Mehrkhodavandi, P. Mechanism of Living Lactide Polymerization by Dinuclear Indium Catalysts and Its Impact on Isoselectivity. *J. Am. Chem. Soc.* **2012**, *134*, 12758–12773.

(98) Nomura, N.; Akita, A.; Ishii, R.; Mizuno, M. Random Copolymerization of ϵ -Caprolactone with Lactide Using a Homo-salen–Al Complex. *J. Am. Chem. Soc.* **2010**, *132*, 1750–1751.

(99) Kan, C.; Ma, H. Copolymerization of L-lactide and ϵ -caprolactone catalyzed by mono- and dinuclear salen aluminum complexes bearing bulky 6,6'-dimethylbiphenyl-bridge: random and tapered copolymer. *RSC Adv.* **2016**, *6*, 47402–47409.